UFL/COEL/MPR-2001/002

OBSERVATIONS OF THE FORMATION AND MAINTENANCE OF BEACH CUSPS ON DEL MONTE BEACH IN MONTEREY, CALIFORNIA

by

GREGORY CHAD MILLER

MASTER'S PROJECT REPORT

2001

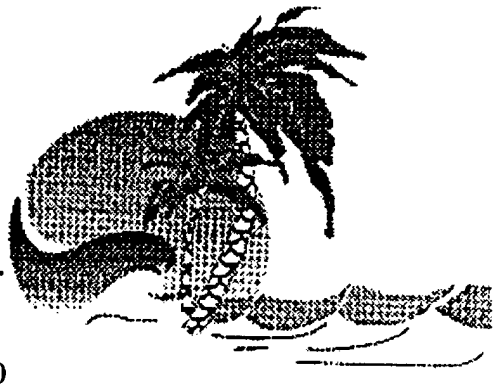

Coastal & Oceanographic Engineering Program
Department of Civil & Coastal Engineering
433 Weil Hall •P.O. Box 116590 • Gainesville, Florida 32611-6590

UNIVERSITY OF FLORIDA

OBSERVATIONS OF THE FORMATION AND MAINTENANCE OF BEACH CUSPS ON DEL MONTE BEACH IN MONTEREY, CALIFORNIA

By

GREGORY CHAD MILLER

AN ENGINEERING REPORT PRESENTED TO THE DEPARTMENT OF CIVIL AND COASTAL ENGINEERING OF THE UNIVERSITY OF FLORIDA IN PARTIAL FULFILLMENT OF THE REQUIREMENTS FOR THE DEGREE OF MASTER OF ENGINEERING

UNIVERSITY OF FLORIDA

2001

ACKNOWLEDGEMENTS

I would like to sincerely thank Jamie MacMahan for all of his assistance with data collection and data analysis for this report, and for getting me out of about of about seven weeks of classes (Linear Waves, Data Analysis) for field work. Although, I guess I'll forgive him for asking questions (tides?) during my defense.

When beginning my master's research, I had no idea what I wanted to study, but I was very interested in being able to work in the field. By working with Jamie on the waverunner and other projects, I was able to assist with field research in Myrtle Beach, South Carolina, Daytona Beach, Panama City, and Anna Maria Island, Florida, and Monterey, California. Some of my "favorite" moments in the field included flooding a $14K "loaner" ADCP, being "dropped" 75 yards offshore to swim in from a surf zone bathymetric survey, "rubbing" the beams of the ADCP (for what felt like hours), and finally tipping the waverunner in the California surf when instrumented with $85K in equipment—"the GPS antenna has a 'small' hole." The five weeks in Monterey were especially educational and ultimately lead to the idea for this report. However, I never thought that going to the beach everyday could ever be an bad "deal", but, after five weeks of Monterey in April, I've changed my mind.

I also want to thank Dr. Ed Thornton of the Naval Postgraduate School (NPS) for (allegedly) funding my participation in the Monterey RIPEX experiment, and for providing the lovely accommodations at the NPS beach "Bed & Breakfast" (a.k.a. abandoned wastewater treatment plant). Jamie and I felt so fortunate to be participating in this experiment that even the lack of heat and hot water in the "B&B" could be overlooked.

Finally, I would like to thank my advisor, Dr. Robert Thieke, for his assistance and direction and, especially, for the 11th hour edits of this report. I would also like to thank Dr. Robert Dean and Dr. Ashish Mehta for serving on my supervisory committee.

TABLE OF CONTENTS

LIST OF TABLES

LIST OF FIGURES

Abstract of Engineering Report Presented to the Department of Civil and Coastal Engineering of the University of Florida in Partial Fulfillment of the Requirements for the Degree of Master of Engineering

OBSERVATIONS OF THE FORMATION AND MAINTENANCE OF BEACH CUSPS ON DEL MONTE BEACH IN MONTEREY, CALIFORNIA

By

GREGORY CHAD MILLER

December 2001

Chair: Dr. Robert Thieke
Major Department: Department of Civil and Coastal Engineering

During the period of 5 April 2001 – 16 May 2001, topographic surveys of Del Monte beach in Monterey, California, were performed on a regular basis to record changes in beach cusp development for comparison to wave data being collected by the Oceanography Department of the Naval Postgraduate School. The surveys were conducted with a Real Time Kinematic Global Positioning System (RTK-GPS) secured to an all-terrain vehicle (ATV). The surveys were performed by driving the ATV on longshore transects of the beach to measure the vertical variation. From these surveys, the size and shape of the cusps were determined for each survey, and cusp variations between surveys were compared to the changes in wave conditions. Cusp spacing was determined through spectral analysis of the survey data, which produced peaks at the primary longshore wave numbers of the surf zone and swash cusps. The field data were then compared to current theory regarding beach cusp formation and maintenance in an attempt to determine the causative, maintenance, and destructive mechanisms.

CHAPTER 1
INTRODUCTION

While participating in the Naval Postgraduate School's rip current (RIPEX) and steep beach experiment in April 2001, dramatic changes in the upper beachface were observed over a relatively short period of time. On one day, beach cusps, which are rhythmic longshore features, were very prominent with a well-established spacing, but, on the next, the vertical relief was greatly diminished with a much less obvious longshore spacing. This dramatic change sparked an interest in the cause of these relatively rapid shoreline changes. Since GPS beach surveys were already being performed to record the nearshore bathymetry and beachface topography during RIPEX, more frequent beach surveys were performed to record any additional changes in the shoreline.

Beach cusps have long been of scientific interest to coastal engineers and geologists, but, from the first descriptions of beach cusps, there have been many apparently contradictory observations and theories. Beach cusps have been observed to form in many types and sizes of sediments ranging from fine sand to large cobblestones (Johnson, 1910) to even large boulders (Butler, 1937). They are generally characterized by steep gradient, seaward-pointing cusp horns and gentle-gradient, seaward-facing cusp embayments. Figure 1-1 defines typical beach cusp features.

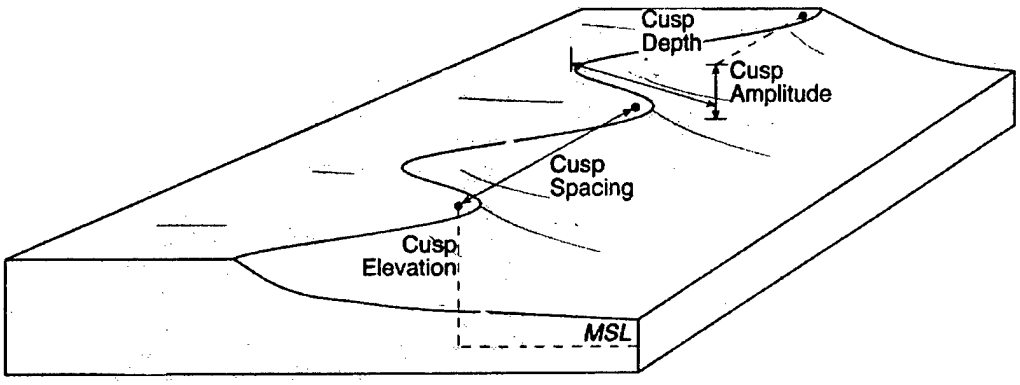

Figure 1-1: Definitions of beach cusp features (Nolan et al. 1999)

Cusps are often regularly spaced, with spacing ranging from centimeters to hundreds of meters. Dolan and Ferm (1968) proposed the hierarchical grouping of coastal features listed below:

(1) cusplets (1.5 m)
(2) typical beach cusps (8 – 50 m)
(3) storm cusps (70 – 120 m)
(4) giant cusps or shoreline rhythms (700 – 1500 m)

The cusps observed at Del Monte Beach were "typical beach cusps" with an average spacing of approximately 35 – 40 meters.

A review of the relevant theories and proposed mechanisms for the formation and maintenance of beach cusps is presented in the following chapter. A more detailed description of the Monterey experiment sites and data collection techniques are presented in Chapter 3, and data analysis techniques are further discussed in Chapter 4. Since there is no universally accepted causative or destructive mechanism for beach cusps, in Chapter 5 this report will compare the collected wave and survey data with the prevailing theories in an attempt to determine the factors that lead to the formation, maintenance, and destruction of beach cusps. Finally, conclusions are presented in Chapter 6. Because beach cusp changes can be readily observed and measured, gaining further understanding of these processes may present additional insight into the more interesting problems of surf zone hydrodynamics and sediment transport.

CHAPTER 2
LITERATURE REVIEW

Johnson (1910) developed one of the first comprehensive theories of the origin of beach cusps and described many of the details of the physical parameters associated with beach cusps. The factors that he considered significant in determining the spacing between cusps were wave height and possibly beach slope, while tidal stage, wind direction and wave period were found to have little impact. As wave height increased, cusp spacing was found to increase as well. Johnson suggests that doubling the height of waves close to the shoreline results in a doubling of cusp spacing. He found that within a series of cusps, the spacing or distance between individual cusps was somewhat regular. However, Johnson also observed that irregularities in spacing were more predominant in the early stages of cusp development. According to Johnson, in order for cusps to form properly, the wave fronts of cusp forming waves must be nearly parallel to the beach. He also noted that cusp origin was associated with irregularly spaced depressions in the beach. Selective erosion by the swash developed from initial depressions in the beach, which the swash would run up and then return along the horns. The ultimate size of these troughs was proportional to the size of the waves, and determined the relatively uniform spacing of the cusps, which developed on the intertrough higher elevations. Equilibrium was established when adjacent channels were of approximately the same size and at the same time of a size appropriate to accommodate the volumes of water traversing them.

Escher (1937) conducted wave tank experiments in an attempt to determine the origin of beach cusps. Escher obtained cusp-like features on a laboratory beach composed of sand. He postulated that a standing wave situated along a wave crest, which was parallel to the beach, would produce areas where greater or less erosion would occur. The spacing of the cusps produced would vary depending upon the wave number of the standing waves. Escher reported that bays flanked by protruding peninsulas offer favorable conditions for this type of wave patterns.

Shepard (1938) observed that cusp formation was more closely related to tidal variation than to changing wave conditions, although he did not state that tides formed the cusps. He observed at high tidal ranges the beach cusps were destroyed and then reappeared at low tidal ranges.

Evans (1938) stated that cusp formation was consequence of the height, character, and duration of the incident waves, and that cusp spacing was a function of wave height. He also noted through field observations on Lake Olga, Quebec, that cusps formed regardless of the angle of incidence, and that the cusp horn indicated the direction of incidence in juvenile cusps. He observed that whenever the proper conditions were present, formation was very rapid, almost instantaneous. It was also his contention that once a cusp had formed, a considerable change in wave conditions was required to destroy it. Initially, Evans postulated that beach cusps were originated by the swash breaking through a beach ridge, which is a long obstruction parallel to the shoreline. Cusps formed preferentially in recently built beach ridges that had been broken through by waves. A very close adjustment existed in the relationship between height and uniformity of waves and that of height and shape of the ridge on which it acted. In a later paper, Evans (1945) modified his early theory of formation to include a more complete explanation of the regularity of spacing between cusps. After the waves broke through the sand ridge, which Evans considered necessary for cusp formation, the parabolic swash and backwash carved out a system of bays and horns. This process continued until equilibrium was obtained with all cusps being relatively the same size.

Bagnold (1940) conducted wave tank experiments on beach formation by waves, and observed the water to be deflected by the cusp horns on the uprush and to return down the center of the embayment, thus contradicting Johnson's observations. Figure 2-1(A) demonstrates Bagnold's observed swash pattern.

Kuenen (1948) developed a theory similar to that of Johnson (1910). He noted that the horns were depositional areas where the material being removed from the bays was deposited. In

Kuenen's theory, as in Johnson's, cusp growth commenced at natural depressions in the beach. Refraction of the swash as it swept into the embayments and fanned out onto the sides of the protruding horns was an essential element in the production of cusps. This caused sediment to be washed sideways out of the trough onto the horns. Larger material tended to accumulate on the horns while finer material was carried away. As long as the depth of water passing in and out of the bay was able to carry the sediment along, enlargement both vertically and horizontally of the bays continued. As a result, the channel became deeper and wider with steeper sides. When the outer portion of the embayment reached a certain limiting depth, erosion tapered off. Kuenen's observed swash flow is depicted in Figure 2-1(B).

The horns were built-up due to refraction of the swash in the embayments and transport of material towards the sides of the bays. Coarse material tended to be pushed back up the beach of the embayment and out along the developing cusps. When the maximum depth in the central area of the bay had been attained, the growth of the bays and horns gradually decreased. Equilibrium was established when the growth potential of all cusps was essentially satisfied.

Eckart (1951) developed a relationship between longshore wavelength, L_e, and period, T_e, of edge waves on a plane beach:

$$L_e = (g/2\pi)T_e^2(2n+1)\tan\beta$$

Longuet-Higgins and Parkin (1962) considered development of beach cusps due to the occurrence of edge waves of the type that can occur on a sloping beach. Although their conclusion was that cusp spacing is not simply related to the period of the waves or the wavelength of low edge waves on a beach, Longuet-Higgins and Parkin developed relationships between mean cusp spacing and wave period, wave height, and swash length. Swash length, as they described it, was the width of the beach between breaking point of the waves and the highest point reach by the swash, averaged over longshore distance and over time. Longuet-Higgins and Parkin determined that the beach cusp data demonstrated a linear relationship between spacing

and maximum swash excursion, which was represented as:

$$\lambda(m) = 2.8 + 0.54\ (\xi_x)_{max}$$

where $(\xi_x)_{max}$ is swash excursion and $\lambda(m)$ is cusp spacing in meters. They found little relationship between cusp spacing and wave period. A close connection between wave height and an even better relationship between swash length and cusp spacing was obtained. The following conditions for the formation of cusps were specified by Longuet-Higgins and Parkin (1962, p. 199);

> "(1) The incident sea waves were always normal to the beach and breakers were long crested.
> (2) The surface material was capable of being shifted freely by the waves but within a few inches of the surface there was always a compact and relatively impermeable layer of material."

Flemming (1964) conducted wave tank experiments in order to investigate the mechanism of transport of particles during cusp formation. He concluded that, in general, each cusp was built on the remains of a predecessor. An impermeable layer was established soon after the swash began to play over the beach. The initial waves eroded the beach surface and washed the fine particles down into the interstices of the underlying material to form an impermeable layer. Cusps then tended to form in the coarse material on top of the impermeable layer.

Flemming observed a water movement pattern in which the swash uprush divided around the horns, flowed into each bay, and then formed a single backwash. This pattern differed from that observed by Kuenen (1948), but agreed with that observed by Russell and McIntire (1965), and Longuet-Higgins and Parkin (1962).

Russell and McIntire (1965) believed that cusp horns were depositional features. The material of cusp horns was found to be softer and coarser that that of the bays. According to them, juvenile cusps began to form during a period of decreasing wave height following an erosional period caused by high waves. Cusps tended to originate and attain maximum development during transitions from winter to summer beach profiles. The cusps having the

sharpest apical points seemed to occur where the impact of waves was parallel to the shore. The more rounded apices developed if there was some longshore drift or slight departure of the wave fronts from a parallel alignment with the shore.

However, the authors did not specify why cusps began to form at one location or another. They simply supposed that cusp formation had begun at some location and described the events that lead to fully developed cusps. The swash arriving at the cusp horn divided and the water swept into the bays. Any material being carried by the upsurge, which did not come to rest, was carried away. Due to the decrease in turbulence and velocity of the water as it flowed around and sometimes over the horns, the heavier and coarser entrained material was deposited there. After the initial removal of loose material from the embayments, the water flowing back down the bays possessed sufficient transportation velocity to keep its suspended load in motion, but rarely was it capable of entraining new load across the bay-floor pavement. This pavement was initially established at the bottom of the bay when all loose materials had been removed by overflowing waters and was resistant to any further loss of material.

Juvenile cusps were irregular at first, about two to three times larger than final cusp spacing. The regularity increased as cusps became better developed. Cusp forming processes apparently succeeded in shifting the original horns so those irregular members became incorporated into larger members.

Bowen and Inman (1969) investigated the nearshore circulation of water on a plane beach exposed to uniform wave train. The wave train when normally incident on the beach generated standing edge waves of the same frequency as the incoming waves. These edge waves interacting with the incident waves produced a steady circulation pattern consisting of onshore flow directed toward the breakers, a longshore current in the surfzone, and an offshore flow in narrow rip currents. Bowen and Inman theorized that the combined flow associated with the incoming waves, the edge waves, and the nearshore circulation pattern would rearrange the beach sediment to produce a regular longshore pattern of cusps. At locations where the surfzone is wide and the

slope of the beach is small, the spacing of cusps is much smaller than the rip current spacing. Although several different types of edge waves may occur on beaches, the subharmonic edge wave, which has a period twice that of the incident waves, is the most easily excited. Slow onshore flow between the rip currents deposits sediment within the surfzone and the seaward flowing rip current erodes a channel. This should result in a system of cusps whose spacing is equal to the wavelength of the nearshore circulation and dominant edge wave.

Komar (1971) theorized that cusps develop in the lee of rip currents, and that once cusps were produced an equilibrium condition would be achieved and the rip currents would disappear. A current cell composed of two rip currents, associated longshore currents, and drift through the breaker zone was proposed. It was expected that cusp development would occur at the center of the cell midway between the rips, but this was not supported in the laboratory and Komar was uncertain if this occurs in nature. Laboratory experiments revealed that cusps formed in the lee of the rips and not in the center of the cell. Apparently, a back eddy shoreward of the rip permits deposition of a lee-rip cusp. The critical factor is believed to be the amount of sand deposited compared to the amount of sand carried out in the rip. Komar states lee-rip cusps are definitely observed in nature. Following the formation of cusps, an equilibrium condition would be attained in which the longshore currents cease and the rips completely disappear. Equilibrium would be reflected by the presence of small waves at the point of the cusps and large waves in the embayments. Komar concludes that the two driving forces necessary for development of this type are (1) a nearshore cell circulation, and (2) longshore currents with an oblique wave approach. Both of these currents would balance and cease to exist at equilibrium.

Guza and Inman (1975) conducted laboratory and theoretical studies of edge waves and the formation of beach cusps and found that the most easily excited edge wave is a zero-mode edge wave with a period of twice that of the incident wave period. This theory indicates that cusp embayments are scoured out at the locations of the edge wave antinodes, whereas cusp horns

occur at the edge wave nodes. This subharmonic edge wave was hypothesized to result in a cusp wavelength of one-half the edge wavelength:

$$\lambda_c = (g/\pi)T_i^2 \tan\beta,$$

where T_i is incident wave period and tan β is beach gradient. Guza and Inman also discuss the possible importance of "synchronous" edge waves of period equal to the incident wave period in cusp formation. In the laboratory, they found the synchronous mechanism to be a higher order, weaker resonance than the subharmonic type.

Kuenen (1948) and others have presented arguments that higher waves result in larger cusp spacing. Dalrymple and Lanan (1976) postulated that this large wave/large cusp spacing may simply be related to the observation that the higher the wave, the longer the wavelength.

Huntley and Bowen (1978) conducted a study of nearshore current velocities, and observed cusp formation during the period of their experiment. Velocity spectra sampled showed energy at subharmonic frequencies preceding the formation of the foreshore cusps. This subharmonic peak persisted for several hours, and exhibited a phase relationship between vertical and horizontal velocity components consistent with a zero-mode, standing, subharmonic edge wave. The mean spacing between cusps also matched the predicted wavelength of a cusp formed by a subharmonic edge wave. Huntley and Bowen were also able to make their cusp-edge wave association due to the observation of energy at the appropriate frequency near the shoreline compared to the more typical assumption of edge wave presence through the use of the incident wave period.

Dean and Maurmeyer (1980) suggested that cusp spacing is linearly related to maximum swash excursion. They stated that the most effective beach cusp development occurs when the wave and swash period are nearly equal. In this case, the backrush flow destructively interferes with the succeeding uprush at the embayment positions of the cusps. Swash period can be approximated by:

$$T_n = 2V_0/(g\sin\beta) = \sqrt{((8\xi_{xmax})/g\tan\beta)}$$

where V_0 is swash velocity at origin, β is beach face slope, and ξ_{ymax} is maximum uprush of the water particle. However, they noted that the swash and wave periods do not need to be precisely synchronous since the backrush occurs over a greater time period than the uprush and any significant return flow through the embayments will reinforce this net circulation. This circulation pattern also results in a steeper slope on the horns since little to no destructive backrush transports sediment seaward, while in the embayments the flow is supplemented by flow from the horns and by the reduction of uprush due to interference with the succeeding wave crest and leads to a milder slope.

Dean and Maurmeyer conducted extensive field measurements of beach cusps, but no actual measurements of wave conditions. From these measurements, the authors concluded that larger swash excursions result in greater beach cusp spacing. From this conclusion, they proposed the following relationships for cusp spacing:

$$\lambda_c = 4(\xi_x)_{max}\sqrt{\varepsilon} \qquad (\xi_x)_{max} = V_0^2/(2g\tan\beta) \qquad \varepsilon = (z_h - z_e)/(z_h + z_e)$$

where $(\xi_x)_{max}$ is the maximum uprush of the water particle, and ε is the relative vertical relief of the cusps with elevations referenced to the still water line.

Dean and Maurmeyer also noted that the edge wave theory predicts an increasing cusp spacing with increasing slope. This theory is contrary to the field observations of Trask (1956) which noted a trend of decreasing cusp spacing with increasing sediment size. Since beach slope increases with sediment size (Bascom 1951), swash excursion and cusp spacing would decrease with increasing sediment size. They also noted that if there were a wide range of wave periods and varying beach slopes, it would be difficult to select a single period and slope for the calculations of cusp spacing.

Inman and Guza (1982) specified two types of beach cusps. Cusps formed in the surfzone by the nearshore circulation system are called "surfzone cusps" and may have

wavelengths that range up to hundreds of meters. The basic beach modifications begin underwater and in the surfzone, and eventually modify the shoreline into large cusps with deep embayments and wavelength equal to the circulation cell wavelength. Cusps formed on the beachface by swash and backwash are called "swash cusps". These cusps have wavelengths up to approximately 75 m, but do not change the overall alignment of the beach. They are also most common on steep reflective beaches, where the incident waves produce a substantial surge of swash up the beachface. Inman and Guza concluded that swash cusp wavelengths are set by subharmonic edge waves providing longshore periodic perturbations in bed form on an initially uniform planar beach. However, perturbations are only possible when the incident wave amplitudes are in the range that can excite subharmonic edge waves. According to the authors, cusp amplitude (η_c), which is defined as distance from apex to valley elevation, is determined by the vertical excursions of significant swash run-up motions, and can be estimated from the following equation.

$$0.13 \leq \eta_c/(\lambda_c \tan \beta) \leq 0.25,$$

where η_c is cusp amplitude, λ_c is cusp spacing, and β is beach slope. The authors related cusp steepness ($\eta c/\lambda c$) and beach slope to give upper and lower limits for cusp amplitudes based on the assumption that edge wave activity initiates cusp formation.

However, Inman and Guza also pointed out several sources of potential error in the use of the equations to predict cusp length formed by a subharmonic edge wave as related to incident wave period. Field wave spectra are seldom monochromatic, which makes identification of an specific incident wave period difficult. Cusp wavelength scales are the square of the incident wave period, so small errors in the period may result in large errors in the predicted cusp wavelength. Finally, the choice of beach slope is difficult because natural beaches are rarely planar and the region over which the beach slope should be calculated is poorly defined.

Takeda and Sunamura (1983) conducted field experiments to measure 52 combinations of swash excursion length (ξ) and beach cusp spacing (λ). In their data, they determined that the mean (ξ/λ) ratio was 2.0 with a data peak at 1.7.

Seymour and Aubrey (1985) reviewed existing theories and conducted field experiments at Leadbetter Beach in Santa Barbara, California, in an attempt to propose a coherent conceptual theory on beach cusp formation. The authors proposed that rhythmic cusps formed during relative stillstands of sea level of sufficient duration to permit initial perturbation of beach geometry, and that the regularly spaced cusps acquired their initial spacing from subharmonic edge waves, as derived from the incident wave period and driven by low steepness waves, exhibiting plunging or surging breaking behavior.

Seymour and Aubrey noted that the "Dean and Maurmeyer mechanism envisions accretion on the horns and erosion in the bays and a tendency to reinforce existing cusp topography", which is in good agreement with Inman and Guza (1982). However, Inman and Guza required an initial rhythmic disturbance to predispose the beach face towards cusp formation, and proposed that this initial disturbance was due to subharmonic edge waves. Thus, the authors concurred that an initial perturbation grows under the constructive mechanism described by Dean and Maurmeyer and Inman and Guza until its elevation reaches a limiting value.

The authors also agreed with Wright et al. (1982) that once a cusp spacing has been cut into a beach, it will dominate the mean spacing until a wave event occurs that establishes a radically different beach cusp spacing, until storm waves destroy the existing system entirely, or until beach cusps are completely filled in by cross-shore or longshore sediment transport. Cusp spacing does not casually adjust to existing wave conditions. They also stated that they believed the only morphology required for cusp formation appeared to be a slope, which will support edge wave generation; generally a large slope leading to non-dissipative surf zones.

Werner and Fink (1993) proposed the self-emergence theory that considers random perturbations on the beachface that eventually organize themselves into beach cusps through feedback processes between beachface morphology and swash processes. The authors considered horn divergent swash motion, uprush on the horns with backrush returning through the center of the embayments, characteristic of beach cusp morphology, where positive feedback enhances existing topographic irregularities and negative feedback inhibits morphological change on well-developed cusps. Werner and Fink used computer simulations to demonstrate that cusp spacing, λ, is scaled by the swash excursion length, S:

$$\lambda = f\,S$$

where f averaged 1.7 for the simulated cusps in the model. Several other researchers have also demonstrated that beach cusp spacing is related to the swash excursion length or the size of the incident waves (Johnson, 1910; Evans, 1938; Longuet-Higgins and Parkin, 1962; Williams, 1973; Dean and Maurmeyer, 1980).

Holland and Holman (1996) reported on the Duck94 field experiment at Duck, NC, to determine whether the measured cusp formations were consistent with the theory of cusp formation by either synchronous or subharmonic edge waves. From this data it was concluded that there was no statistical support for the formation of beach cusps by edge waves. However, the authors proposed that swash motions over well-developed cusps at the incident wave frequency could excite edge waves, which would cause a second set of cusps at spacings consistent with edge wave length.

Masselink et al. (1997) proposed that cusp destruction and build-up occurs as a function of the surf similarity parameter, ξ, proposed by Battjes (1974):

$$\xi_1 = (\tan\beta)/\sqrt{(H_0/L_0)}$$

where $\tan\beta$ is the beachface gradient, H_0 is the deepwater wave height, and L_0 is the deepwater wavelength. According to Battjes, when $\xi_1 > 2$, waves do not break but surge up the beach face;

when $2 > \xi_1 > 0.4$, plunging waves prevail; and for $\xi_1 < 0.4$, waves break by spilling. Masselink et al proposed the following relation with the surf similarity parameter using breaking wave height, H_b, instead of deep-water wave height, H_0:

$$\xi_2 = (\tan \beta)/\sqrt{(H_b/L_o)}$$

When $\xi_2 < 1.2$, cusp destruction occurs, while when $\xi_2 > 1.2$, cusp build-up takes place. This threshold suggests that cusp build-up may occur under the influence of both surging and plunging breakers.

Masselink and Pattiaratchi (1998) presented a numerical model simulating the motion of water particles on beach cusp morphology under the influence of an initial velocity and gravity. This model indicated that the typical swash pattern on beach cusps is three-dimensional, with wave uprush diverging at the cusp horns resulting in concentrated backwash streams in the embayments. The authors stated that the degree of horn divergence is a function of the parameter, $\varepsilon(S/\lambda)^2$, where ε quantified the beach cusp prominence:

$$\varepsilon = (\tan \beta_{horn} - \tan \beta_{emb})/(\tan \beta_{horn} + \tan \beta_{emb});$$

and where S was the horizontal swash excursion length, and λ is cusp spacing. When $\varepsilon(S/\lambda)^2 < 0.015$, swash circulation is essentially 2-dimensional (oscillatory) and eventually results in infilling of the embayments. When $0.015 \leq \varepsilon(S/\lambda)^2 \leq 0.15$, wave uprush is deflected from the cusp horns and flows into embayments, and the ensuing swash/backrush reinforces cusp development and maintains existing cusp morphology. When $\varepsilon(S/\lambda)^2 > 0.15$, overtopping of the cusp horn occurs and, as a result, cusp horns are eroded and accretion occurs in the embayments. Destruction of cusp morphology through horn convergent swash flow and overtopping is generally a rapid process, whereas infilling of embayments through oscillatory swash motion is considerably slower.

Masselink and Pattiaratchi also identified five swash flow patterns based on beach cusp morphology and incident waves. Oscillatory swash is largely unaffected by cusp morphology.

Horn divergent swash motion is characterized by wave uprush from the horn to the center of the embayment (Bagnold, 1940; Russell and McIntire, 1965; Dean and Maurmeyer, 1980). Horn convergent swash motion occurs when the swash enters the embayment and fans out onto the sides of the protruding horns and backrush is concentrated at the horns (Kuenen 1948). Figure 2-1 depicts horn divergent flow in (A) as first observed by Bagnold (1940), and horn convergent flow in (B) as observed by Kuenen (1948).

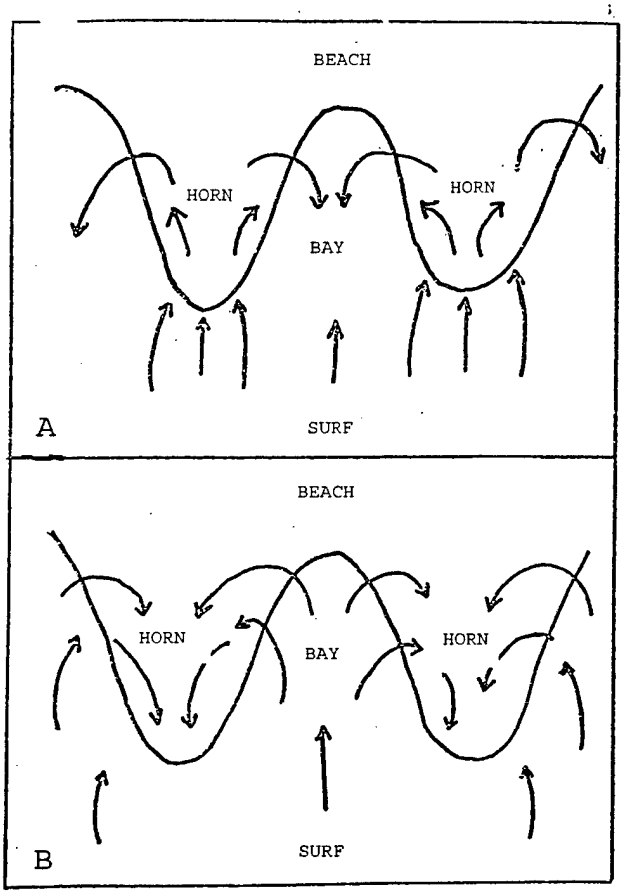

Figure 2-1: Diagrams demonstrating horn divergent flow (A), and horn convergent flow in (B). (Bodie 1974)

According to Williams (1973), swash flow from the embayment to the horn is prevalent under "gentle" swash action, and Dyer (1986) stated that gentle beachface gradients are conductive to inducing horn convergent flow. Both Williams and Dyers attributed this convergent flow to wave refraction. Sweeping swash motion occurs when waves approach the

shore obliquely and induce a significant littoral drift. The swash jet occurs after a strong backwash retards the incoming swash such that a large volume of water is concentrated at the base of the beachface until the uprush breaks through the diminishing backrush as a strong jet up the embayment (Eliot and Clark, 1986). The first three types of swash motion are typical fair weather conditions (Dean number $\Omega < 1$ and $\xi > 1.2$), while the last two occur under more energetic wave conditions and are obviously destructive to beach cusp systems. The authors stated that it is unclear as to how the other three swash motions maintain cusp morphology, but that the uprush/backrush inequality appeared to suggest that only horn divergent flow is capable of maintaining and reinforcing existing beach cusp morphology (Bagnold, 1940; Russell and McIntire, 1965; Dean and Maurmeyer, 1980; Holland and Holman, 1996; Masselink et al., 1997).

Holland (1998) reported on almost 9 years of video imaging data collected at Duck, NC, in an attempt to document the environmental conditions conductive to beach cusp formation and quantify the degree of uniformity of cusp spacing. Holland noted that after close observation of the data that the majority of the cusps formed during the transition from storm to low energy wave conditions as the breaker angle passed through normal incidence. Wave conditions were generally non-dissipative during these events with the surf-scaling parameter, φ, values less than 5.0. The surf-scaling parameter is defined as:

$$\varphi = (H_b/2)*\omega^2/(g\tan^2\beta),$$

where $\omega = 2\pi/T$. Using the entire data set, Holland proposed the following empirical relationship, as a function of storm presence, reflective conditions, and normal incidence, for conditions favorable to cusp formation following within three days of a storm:

$$\cos(3|\alpha_b|)/\varphi \geq 0.16$$

where α_b is breaking angle of incidence, and φ is the surf-scaling parameter.

Holland found no significant linear relationships (defined as r^2 correlation values being significantly different from zero with 95% confidence) between mean cusp spacing (λ) and wave

period (T), incidence angle (α), beach slope (β), or surf-scaling parameter (φ). However, he did find significant correlation for linear relationships between mean spacing (λ) and both significant wave height (H_s) and breaking wave height (H_b), although the regression explained less than 12% of the total variation about the mean.

Holland's findings support several qualitative statements concerning conditions preferential to cusp development. The data clearly demonstrated that wave incidence must be normal to the beach for cusp formation, as observed by Longuet-Higgins and Parkin (1962). He also observed that reflective wave conditions, as expressed by the surf-scaling parameter, are necessary for cusp formation (Guza and Inman, 1975; Wright et al., 1979). No cusps formed during dissipative conditions, defined as $\varphi > 20$. Holland also stated that a significant dependence on frequency narrow-bandedness was indicated, which Guza and Inman (1975) cited as a possible requirement for cusp formation through the excitation of subharmonic edge waves. The data also showed a clear pattern of cusp formation 2 – 4 days following a peak in storm intensity.

CHAPTER 3
DATA COLLECTION

3.1 Description of Experiment Site

Data collection was performed during participation in RIPEX, a rip current experiment hosted by the Naval Postgraduate School, Monterey, California, during the months of April and May 2001. The beach cusp investigation occurred on the center and northern ends of Del Monte Beach in Monterey, California. The incident waves were energetic, narrow-banded, and near-normally incident due to sheltering by headlands and strong refraction due to Monterey Canyon. After further research, this site also corresponded to the sites of experiments conducted by Smith (1973) and Bodie (1974). From Bodie (1974), this site exhibits essentially no longshore current. During the experiment, the average swell for this area was from the NNW with a period of approximately 10 seconds and a deep water wave height of 0.9 m. The tide was mixed, predominantly semi-diurnal with a mean range of approximately 2 m. Figure 3-1 shows the general location of Monterey Bay in California, as well as the locations of the four experiment sites; North and South RIPEX sites, Site 3 and Site 4.

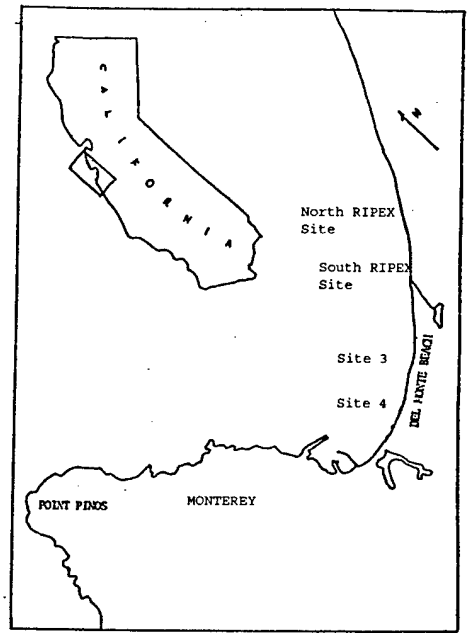

Figure 3-1: Monterey Bay and experiment sites

Del Monte Beach exhibited a significant wave height gradient due to refraction from north to south with the largest waves at the north end. Thus, cusp formation could be observed over a wide range of wave conditions. Unfortunately, no simple relationship exists between the wave heights observed at various locations along the beach due to the changing refraction pattern associated with the incoming deep water wave angle and wave period.

The site also exhibited a gradient in sand sizes along the beach from north to south. According to Smith (1973), the sediment at the north end of the beach is a medium sand, while at the south end of the bay, the sand is a fine sand. Due to this sediment variation, the beach has a range of slopes varying from approximately 7 - 8 degrees at the north end to approximately 3- 4 degrees at the south end of the experiment site.

3.2 Data Collection Techniques

During the period of 5 April 2001 to 16 May 2001, the beach was mapped using fourteen Real Time Kinematic Global Positioning System (RTK-GPS) surveys. This survey method provides 1 – 3 cm horizontal accuracy and 3 – 5 cm vertical accuracy. GPS positioning technology can be classified as navigational or survey grade. Navigational GPS, including both autonomous and differential GPS (DGPS), is based on a time-of-flight measurement known as pseudoranging. Survey-grade or geodetic GPS is based on a technique where two or more GPS receivers record the phases of the carrier waves emitted by four or more GPS satellites. When the distances between the stations are large, several hours of GPS observations are required in order to produce a single relative position solution with an accuracy of 1 cm. Geodetic GPS is usually a post-processed and not a real-time approach. However, when the interstation baselines are less than 15 km the geodetic analysis can be simplified to the point that it can be implemented in real-time. With RTK-GPS, a base station is set up at a point with a known position, and it transmits its phase measurement by radio link to the roving GPS receiver. The roving receiver then models these measurements as well as its own to determine the vector between the base station and the

rover. Since the coordinates of the base station are known, knowledge of the baseline vector allows the coordinates of the rover to be determined. Once system initialization has been achieved, determination of rover position typically takes between 1 - 10 seconds.

While RTK-GPS provides coordinates for each of the stations visited by a roving receiver, in reality, it is the relative position of the rover and base station that is being determined. If one were to modify the coordinates assigned to the base station by a small value, the rover's coordinates would shift by the same amount. However, if the nominal position assigned to the base station is in error by more than 10 m, then the baseline vectors calculated by RTK-GPS begin to deform. Therefore, it is best to set up an RTK base station on a monument whose coordinates were previously determined by a static geodetic survey. During this experiment, the base station was set up over benchmarks established by the Naval Postgraduate School. The survey data were collected using a rover unit, consisting of a GPS antenna mounted to a 6-wheel all-terrain vehicle (ATV) to collect the uncorrected positions, a radio to receive the corrections determined at the reference receiver, and a libretto laptop computer to control the survey and store the corrected data points. The RTK-GPS sampled at a rate of 5 Hz and the rover was typically driven at a speed of 4 m/s – 5 m/s.

Fourteen surveys were conducted were conducted along a 1000-m section of beach at the north end of Del Monte Beach, corresponding to the RIPEX experiment site. These surveys were conducted on 5 April, 14 April, 18 April, 23 – 27 April, 29 – 30 April, 5 May, 8 May, 13 May, and 16 May. This site had the steepest beach slope with an average of approximately 7 degrees, and the most energetic wave conditions. Six beach surveys were conducted along the entire length of Del Monte Beach, covering approximately 2500-m. These surveys were conducted on 24 – 27 April, 29 April, and 30 April. The beach surveys were performed by making longshore transects with the ATV from the swash zone to the upper beach face as close to the time of low tide as possible. Surveying at this time allowed collection of data both above and below the area of primary interest, the high tide swash zone. Each survey consisted of an average of 11

longshore transects over an average beach width of 45-m. Additional transects were also performed during these days to further map the beach cusp horns and embayments. During these transects, the ATV was driven down the cusp horn and up through the center of the embayment to record the cusp maximum and minimum elevations.

Wave data were collected by the Oceanography Department of the Naval Postgraduate School during the RIPEX experiment. A directional wave buoy was located 10 km offshore to measure incident deep water waves. Nearshore wave height and period were measured by a three-velocity-component Acoustic Doppler Velocimeter (ADV) in approximately 6-m water depth.

CHAPTER 4
DATA ANALYSIS AND PRESENTATION

4.1 Survey Data Analysis

The RTK-GPS raw data for each of the 14 surveys were converted to a local x-, y-, z-coordinate frame with the x-, y- datum located at the survey benchmark of 36°37'00.3710 N, 121°51'09.2225 W, and the z- datum from the local geoid elevation, which approximates mean sea level. Once this conversion was made, the longshore RTK-GPS transects were plotted in the local reference frame, where x- represents cross-shore distance increasing offshore. The x-component ranges from 10 m – 50 m at the North RIPEX site at the northern-most end of the experiment. The y-component represents the longshore distance, increasing from north to south. This value ranges from –350 m at the north end to 2150 m at the southern-most end of the experiment site. A plot of the converted data showing transit lines from 14 April is presented in Figure 4-1 below:

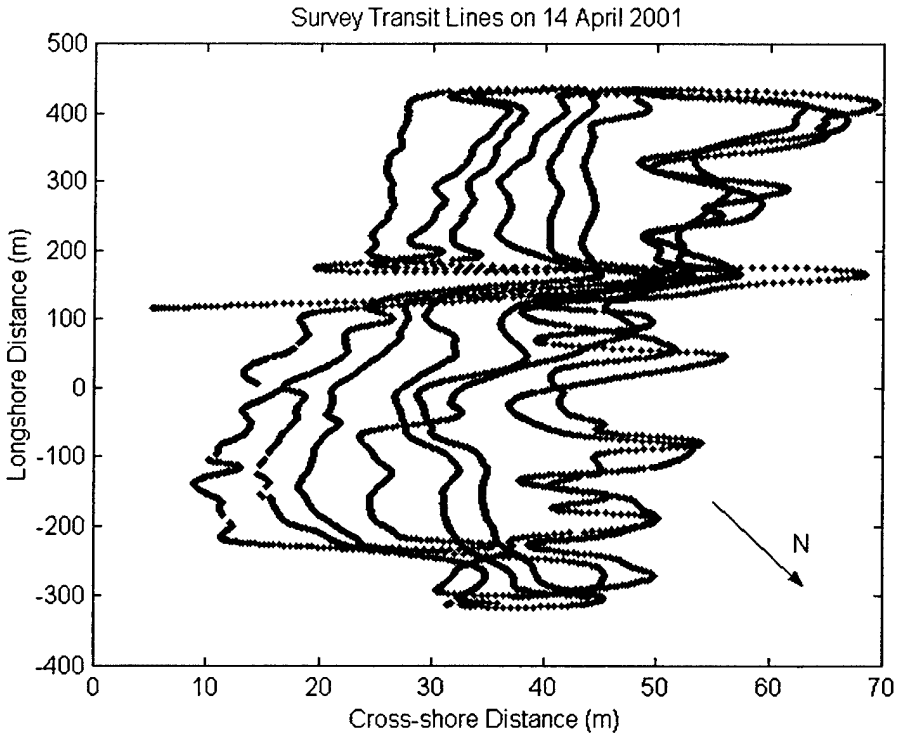

Figure 4-1: Survey transit lines from 14 April 2001 at North and South RIPEX sites

The transects on the upper beachface (10 m – 30 m) generally remained parallel to the shoreline, while the transects in the swashzone (30 m – 50 m) tended to follow the swash excursion due to wave avoidance during surveying. The MATLAB program for this data conversion was provided by Jamie MacMahan, PhD candidate at the University of Florida.

The converted data from each of the RTK-GPS surveys was also plotted as a contour map of the beachface to qualitatively demonstrate the beach changes over the survey period. An example of the topographic plot of the northern end of the beach, the North and South RIPEX sites, on 14 April 2001 is provided in Figure 4-2.

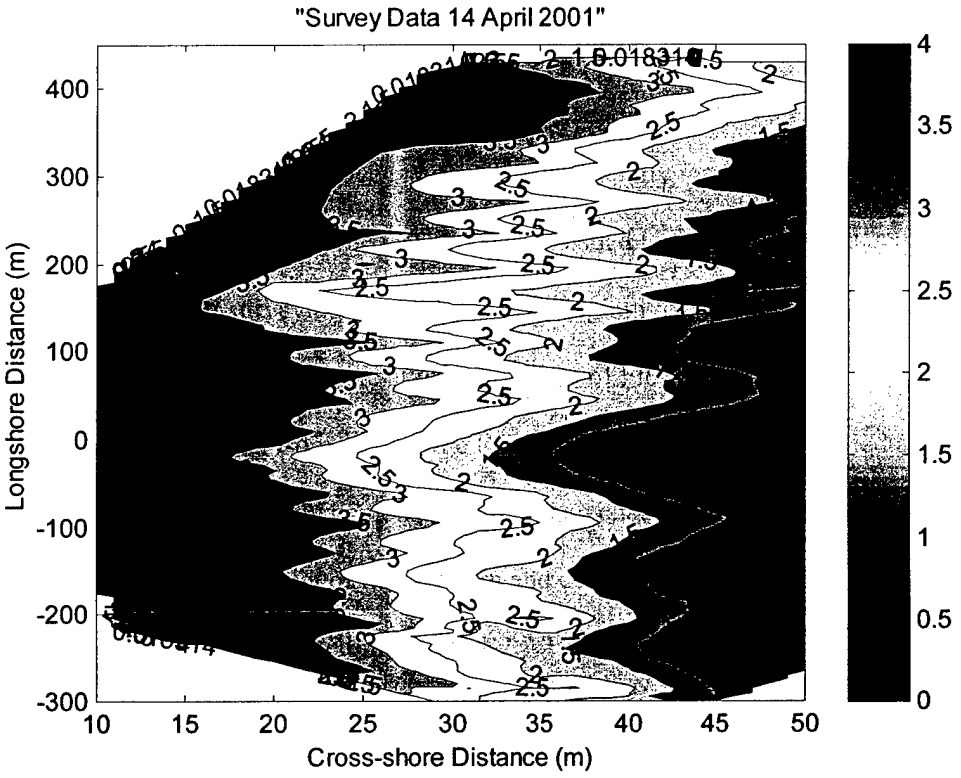

Figure 4-2: Beachface topography from survey data on 14 April 2001 at North and South RIPEX sites

The swash cusp horns can clearly be seen as the protrusions extending from the 3.0 m contour line out to the 1.5 m contour line in some cases. The larger surf zone cusp horns can also be seen as the protrusions extending from the 1.0 m and 0.5 m contour lines with spacing on the order of 100 m.

To demonstrate the changes in the beach face over the survey period, the topographic plot of the same portion of the beach face on 16 May 2001 is provided in Figure 4-3 below.

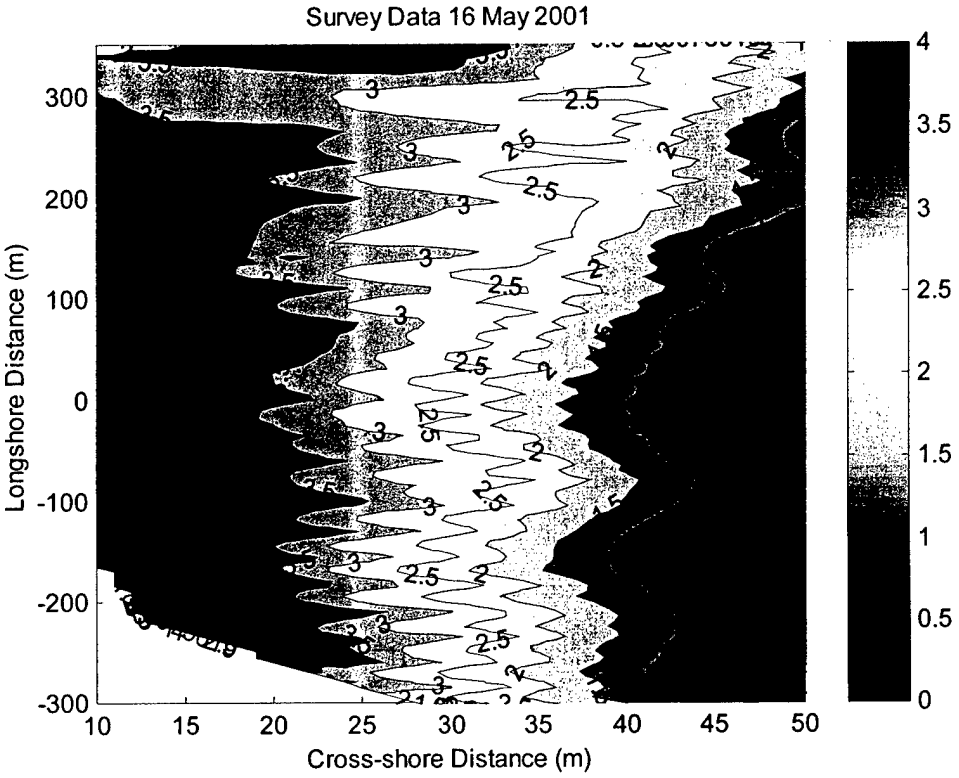

Figure 4-3: Beachface topography from survey data on 16 May 2001 at North and South RIPEX sites

Over the five week survey period, the cusp spacing decreased from an average spacing of about 35 m – 40 m in mid to late April to between 25 m – 28 m by the middle of May. As will be shown later, the 35 m – 40 m cusp spacing remained stable at the North and South RIPEX sites until a storm event occurred in early May. That event changed the cusp spacing to the system depicted in the 16 May survey. Qualitatively comparing each of these topographic plots, the general changes in the beach face and specifically beach cusp spacing can be observed over the course of the five week survey period. The topographic beach surveys for the remaining survey dates are included in Appendix A.

However, in order to quantitatively determine the average cusp spacing from each survey date, the average longshore cusp spacing was calculated from the wave number spectrum, where

wave number was defined as reciprocal wavelength of the longshore variation in the measured vertical position at an estimated fixed cross-shore distance relative to the shoreline. The average cusp spacing was then defined as the wavelength corresponding to the local peak in spectral density.

4.1.1 North & South RIPEX sites

At the North RIPEX site, -350 m ≤ y ≤ 0 m, these longshore cuts were made at the arbitrary cross-shore distances of 20 m, 25 m, 30 m, 35 m, and 40 m. Beyond the longshore distance of 0 m, the bay begins to curve to the west, so making cuts at fixed cross-shore distances was no longer possible to maintain a position relative to a fixed baseline. To compensate for this slight curvature, three lines were determined to fit the curve of the bay in order to determine the longshore variation of the vertical position at a fixed cross-shore distance relative to the shoreline. Therefore, the beach was divided into three additional sites for data analysis purposes: South RIPEX Site, 0 m ≤ y≤ 600 m; Site 3, 1000 m ≤ y ≤ 1600 m; and Site 4, 1600 m ≤ y ≤ 2200 m. Figure 4-4 below depicts the entire survey area and demonstrates the curve of the bay.

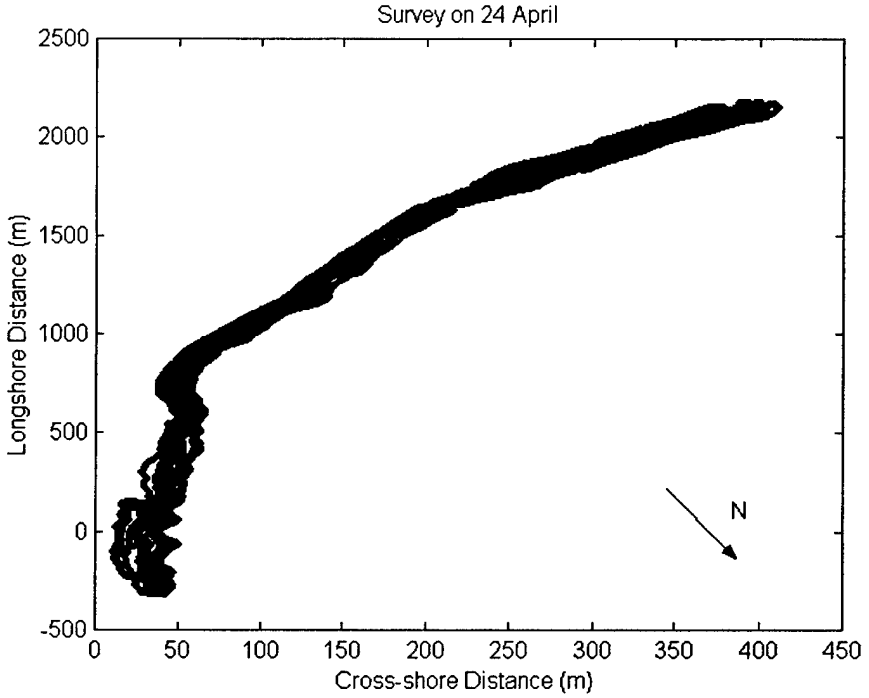

Figure 4-4: Survey transit lines on 24 April 2001 at the North and South RIPEX sites, Site 3, and Site 4

A plot of the detrended longshore transect at 25 m cross-shore on 14 April at the North RIPEX site (-350 m ≤ y ≤ 0 m) and the corresponding spectral analysis is depicted below in Figure 4-5. These data were detrended to remove the effects of beach slope when comparing the spectral analysis of each of the cross-shore cuts.

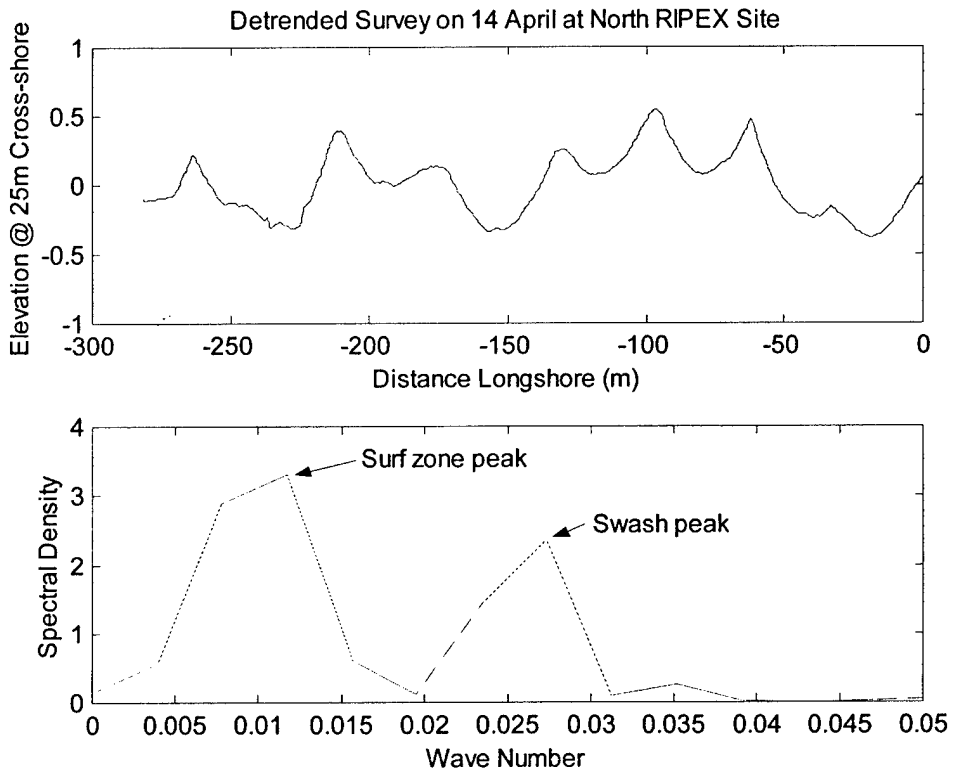

Figure 4-5: Detrended longshore transect at 25 m cross-shore on 14 April at the North RIPEX site and results of spectral analysis showing average surf zone and swash cusp wave numbers

The top plot demonstrates the longshore elevation changes at the 25-m cross-shore distance at the North RIPEX Site. From the bottom plot, the swash cusp peak is at a wave number of 0.0274, or an average cusp wavelength of 36.5 m. Surf zone cusps likely formed from the nearshore circulation system also demonstrate a strong signal with an average wavelength of approximately 105-m.

Similar spectral analysis was performed on each set of survey data, and the results for swash cusp spacing are summarized in Table 4-1 below. The North RIPEX site is defined as the longshore distance from $-350 \text{ m} \leq y \leq 0 \text{ m}$, and the South RIPEX site is $0 \text{ m} \leq y \leq -600 \text{ m}$.

Table 4-1: Summary of swash cusps at North and South RIPEX sites during survey period

Date	North RIPEX Site Primary Spacing	Secondary Spacing	South RIPEX Site Primary Spacing	Secondary Spacing
14 April 01	36.5 m	N/A	42.9m/36.5 m	64.1 m
18 April 01	36.5 m	42.9 m/36.5 m	36.5 m/42.9 m	64.1 m
23 April 01	36.5 m	42.9 m	36.5 m/42.9 m	64.1 m
24 April 01	36.5 m	42.9 m	36.5 m/42.9m	N/A
25 April 01	42.9 m/31.9 m	N/A	42.9 m/36.5 m	N/A
26 April 01	36.5 m/42.9 m	28.6 m	42.9 m/36.5 m	64.1 m
27 April 01	36.5 m/42.9 m	N/A	42.9 m/36.5 m	64.1 m
29 April 01	36.5 m/42.9 m	N/A	42.9 m/36.5 m	64.1 m
30 April 01	36.5 m/42.9 m	N/A	42.9 m/36.5 m	64.1 m
5 May 01	36.5 m, 28.6 m, 21.2 m	21.2 m, 36.5 m, 28.6 m	64.1 m	42.9 m – 31. 9 m
8 May 01	25.6 m/28.6 m	36.9 m	42.9 m	31.9 m – 28.6 m
13 May 01	28.6 m/25.6 m	36.9 m/42.9 m	42.9 m	36.9 m – 28.6 m
16 May 01	25.6 m/28.6 m	36.9 m	42.9 m	36.9 m - 28.6 m

The primary swash zone cusp spacing at the North RIPEX site was fairly constant at 36.5 m from 14 April – 24 April. During these dates at the North RIPEX site, the spectral energy at the 30 m cross-shore cut increased slightly around the wave numbers corresponding to the 36.5 m/42.9 m cusp spacing. There was very little change in the spectral energy at the other

cross-shore distances. The cusp spacing at the South RIPEX site was fairly stable at 36.5 m/42.9 m from 14 April – 24 April. However, there was a general decrease in energy at these wave numbers at the 20 m, 25 m, 30 m, and 35 m cross-shore distances over this time period. The spectral analysis plots at these sites from 14 April – 24 April are depicted in the figures below.

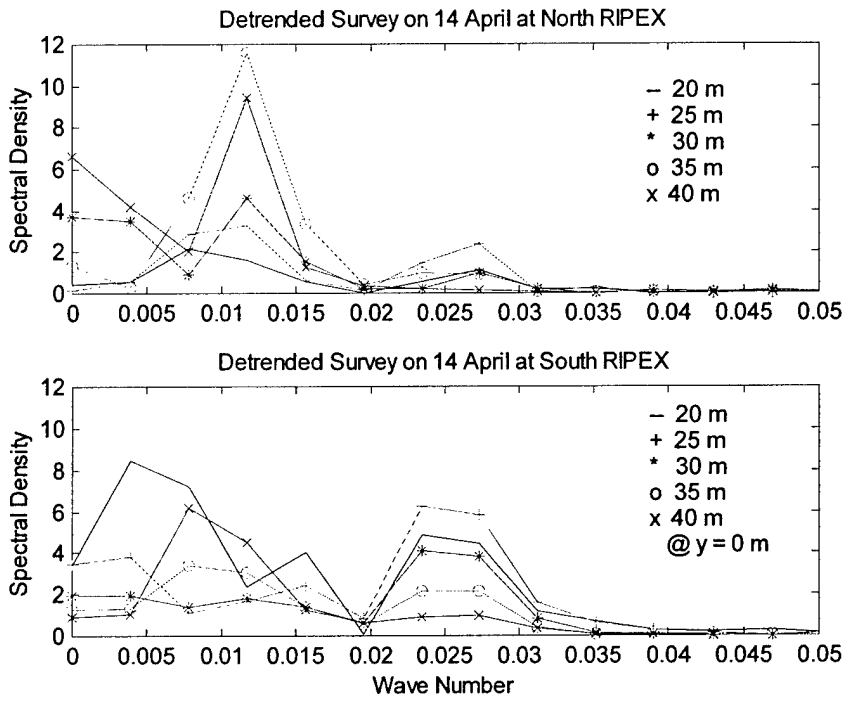

Figure 4-6: Spectral analysis of beach cusp spacing at various cross-shore distances on 14 April 2001

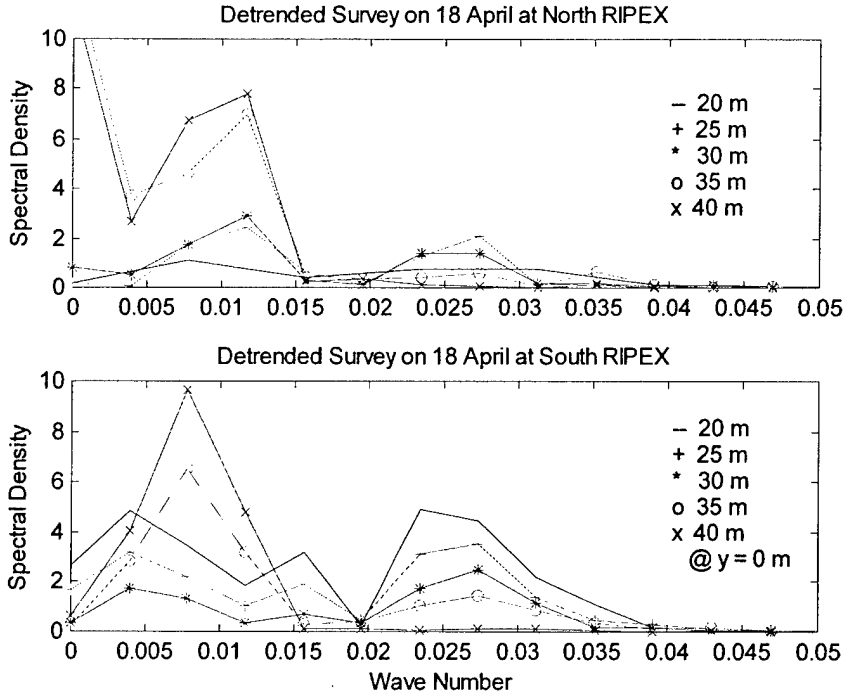

Figure 4-7: Spectral analysis of beach cusp spacing at various cross-shore distances on 18 April

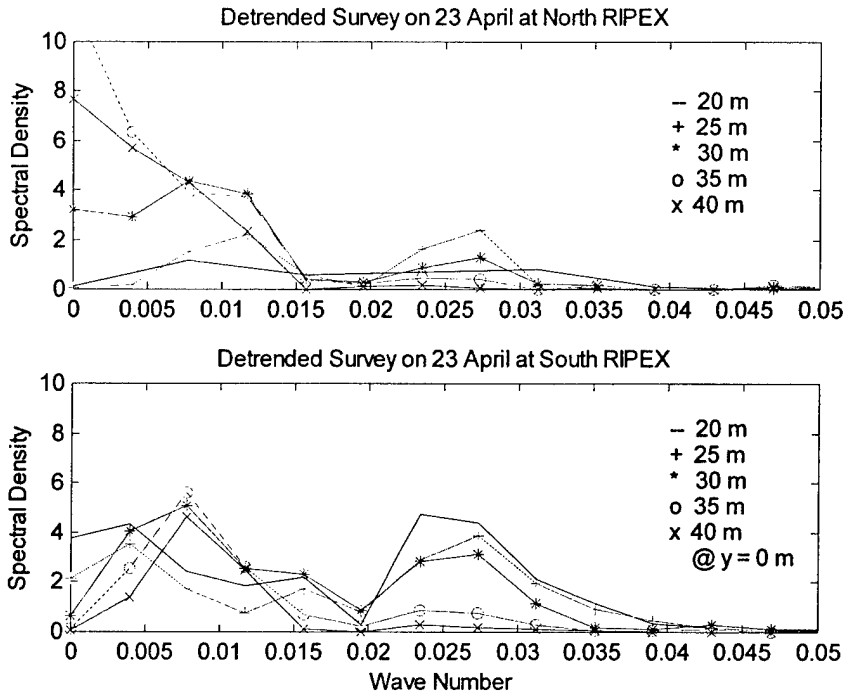

Figure 4-8: Spectral analysis of beach cusp spacing at various cross-Shore distances on 23 April

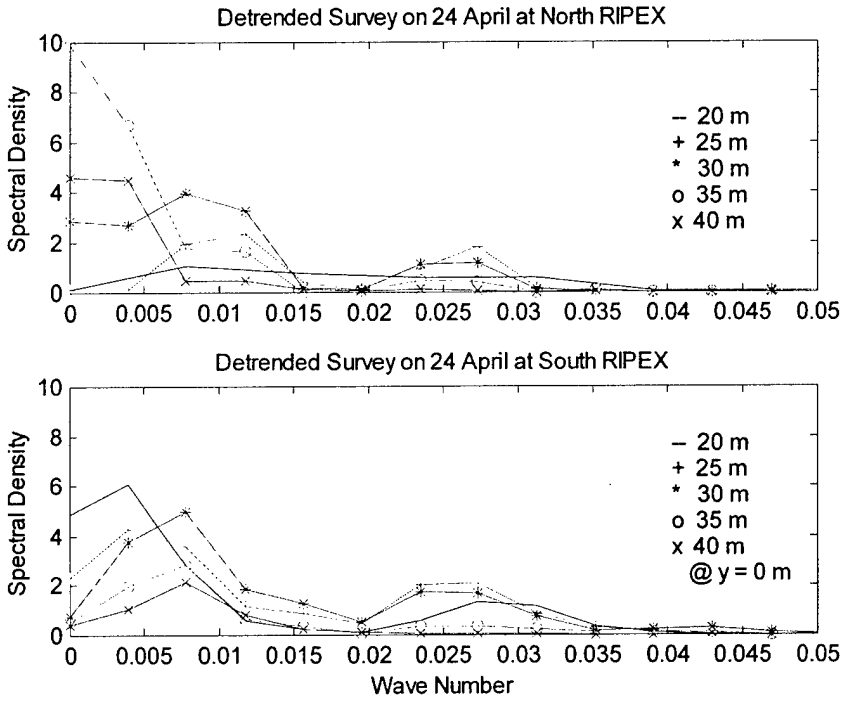

Figure 4-9: Spectral analysis of beach cusp spacing a various cross-shore distances on 24 April

On 25 April, there was a slight dispersion and loss of spectral energy at the North RIPEX site from the 36.5 m spacing to 42.9 m - 31.9 m spacing. A similar trend was observed at the South RIPEX site on 24 April, where the signal was weakened considerably and with a minor shift in the wave number from 0.0274 to 0.0237. On 26 April, the North RIPEX site spacing restabilized at 36.5 m/42.9 m. This spacing was then maintained through 30 April. However, from 26 April to 30 April, there was a considerable strengthening and focusing in the spectral signal around the 36.5 m cusp spacing in the swashzone at distances of 25 m, 30 m, and 35 m cross-shore.

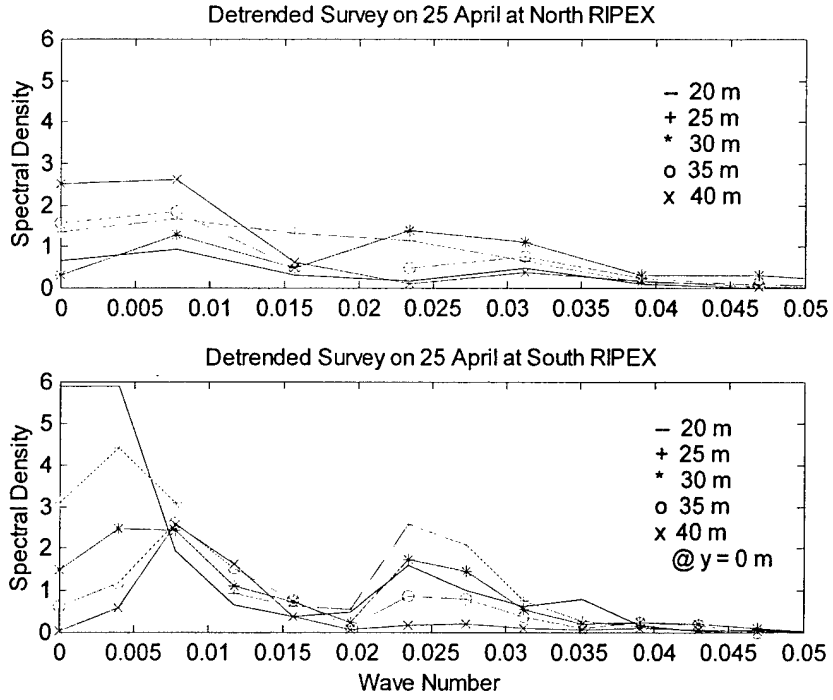

Figure 4-10: Spectral analysis of beach cusp spacing at various cross-shore distances on 25 April.

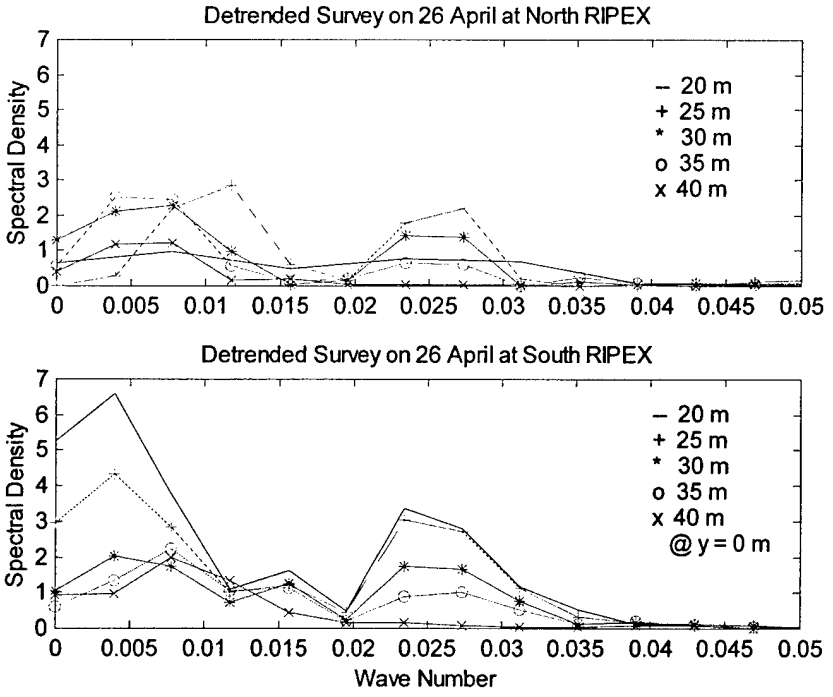

Figure 4-11: Spectral analysis of beach cusp spacing at various cross-shore distances on 26 April

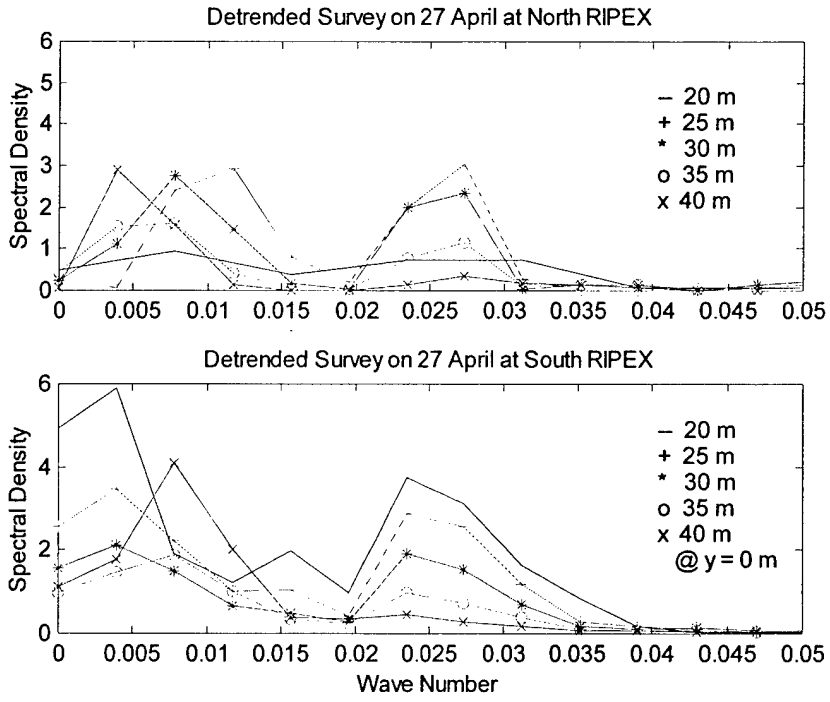

Figure 4-12: Spectral analysis of beach cusp spacing at various cross-shore distances on 27 April

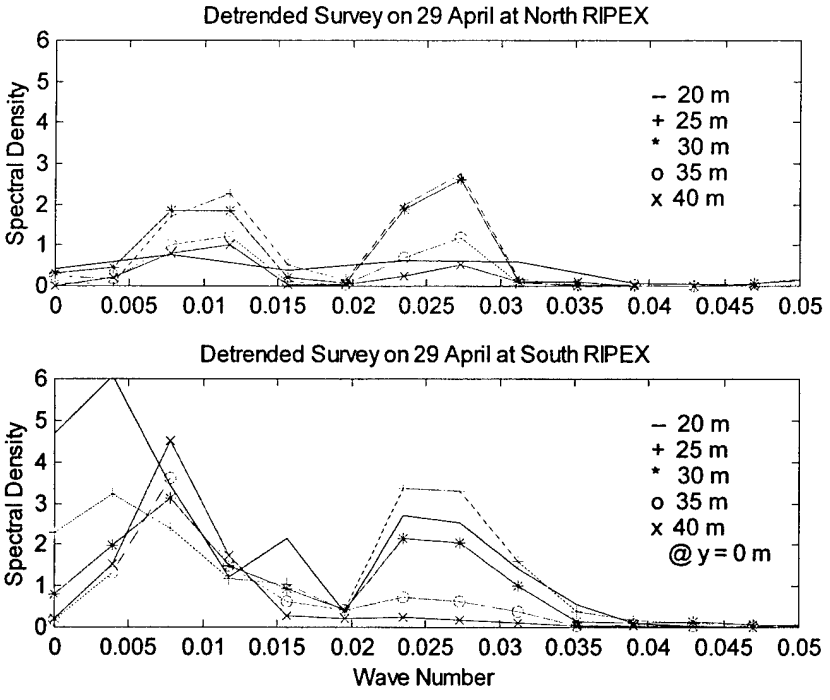

Figure 4-13: Spectral analysis of beach cusp spacing at various cross-shore distances on 29 April

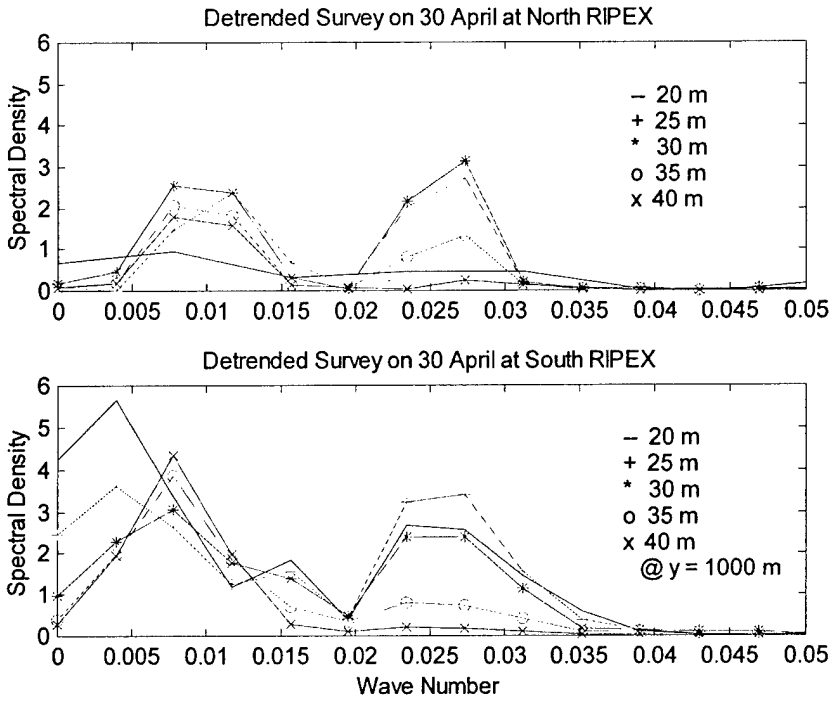

Figure 4-14: Spectral analysis of beach cusp spacing at various cross-shore distances on 30 April

By 5 May, the cusp spacing at both sites had changed dramatically. At the North RIPEX site, the spectral energy dispersed between three wave numbers, representing wavelengths of 36.5 m, 28.6 m, and 21.2 m. On 8 May, the primary cusp spacing had stabilized around the 25.6 m/28.6 m wavelength with an increase in spectral energy at the 25 m, 30 m, and 35 m cross-shore distances. Due to the significant decrease in spectral energy on 8 May, the scale on Figure 4-16 was changed to better depict the observed energy around the swash zone cusp wave numbers. On 13 May, the signal at 30 m and 35 m cross-shore had been reduced, although still focused around the 25.6 m spacing, while the signal at the 25 m cross-shore distance had increased around that same spacing. On 16 May the signal strength had again increased at the 30 m and 35 m cross-shore distances with no effect at 25 m.

At the South RIPEX site, the primary cusp wavelength shifted from 42.9 m/36.5 m to 64.1 m wavelength at 20 m and 25 m cross-shore with a dispersion of energy between the

wavelengths of 31.9 m – 42.9 m. On 8 May, the signal strength increased at the 42.9 m wavelength at 20 m and 25 m cross-shore, but the 20 m signal at the 64.1 m wavelength was considerably diminished. Again, note the change in scale from 5 May. On 13 May, the primary cusp spacing remained at the 42.9 m wavelength at 20 m and 25 m cross-shore, although there was a new peak formed at the 32.2 m spacing at 20 m cross-shore, and the signal at the 64.1 m wavelength continued to weaken. On 16 May, there was a general weakening of signal strength at the 42.9 m wavelength, but the signal at the 32.2 m wavelength increased slightly.

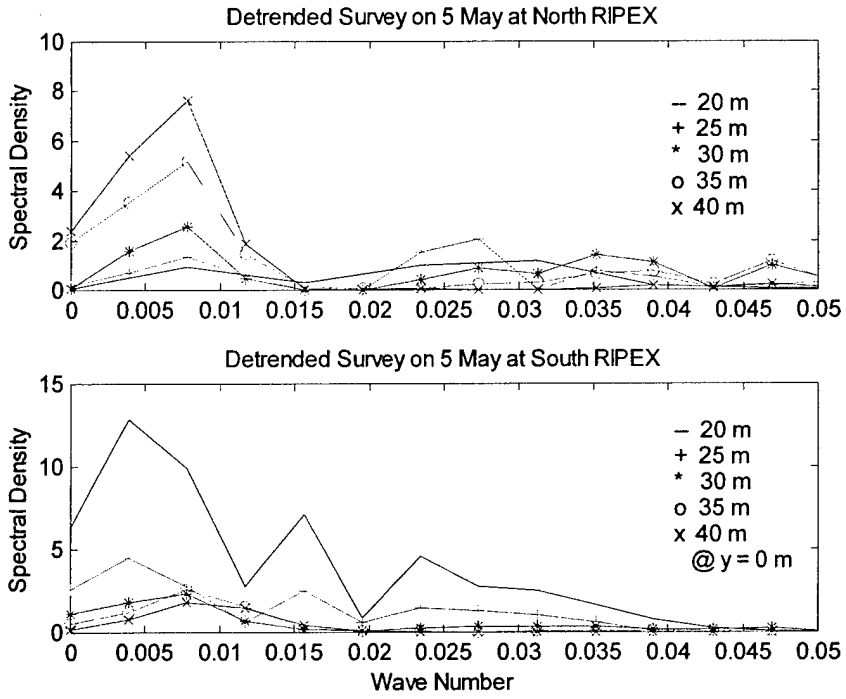

Figure 4-15: Spectral analysis of beach cusp spacing at various cross-shore distances on 5 May

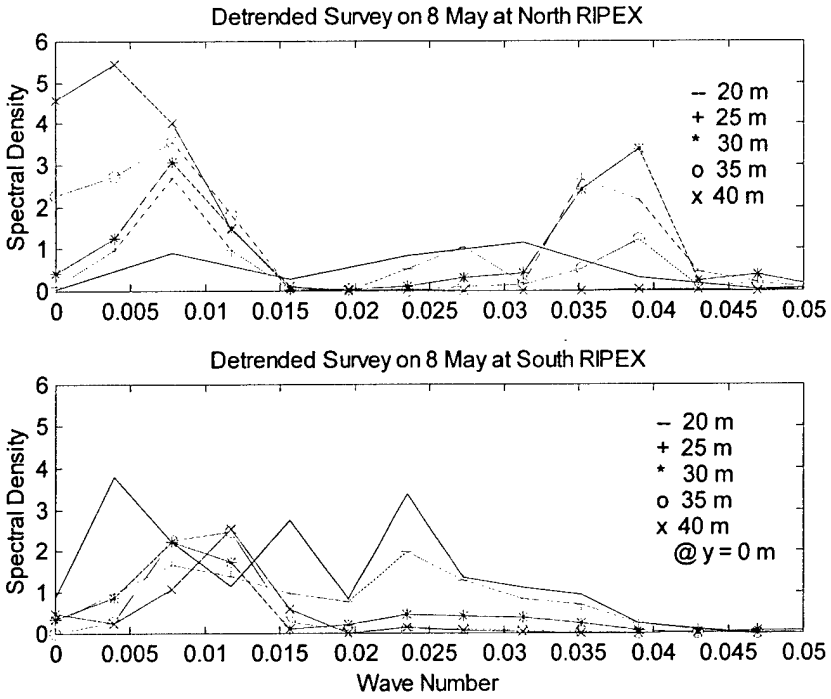

Figure 4-16: Spectral analysis of beach cusp spacing at various cross-shore distances on 8 May

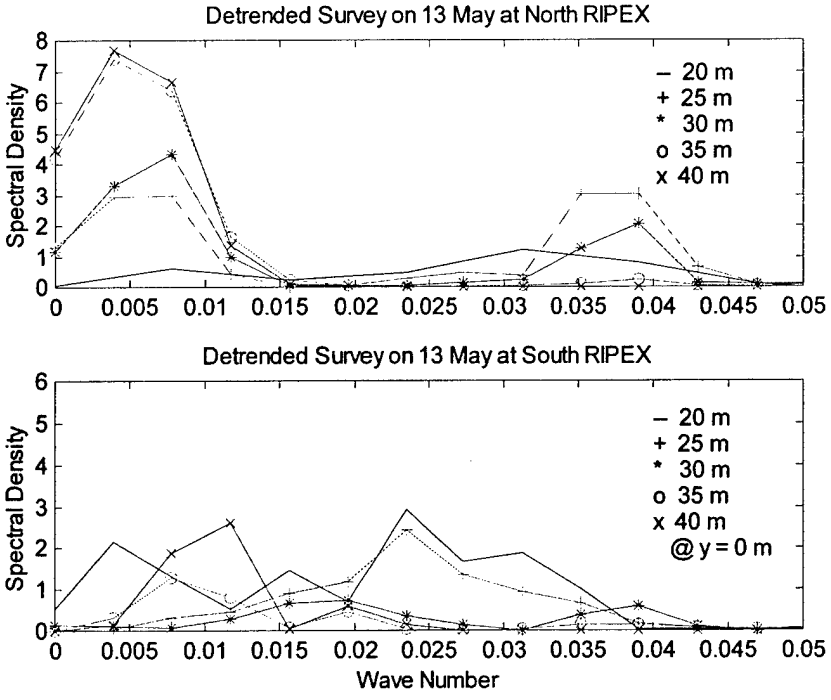

Figure 4-17: Spectral analysis of beach cusp spacing at various cross-shore distances on 13 May

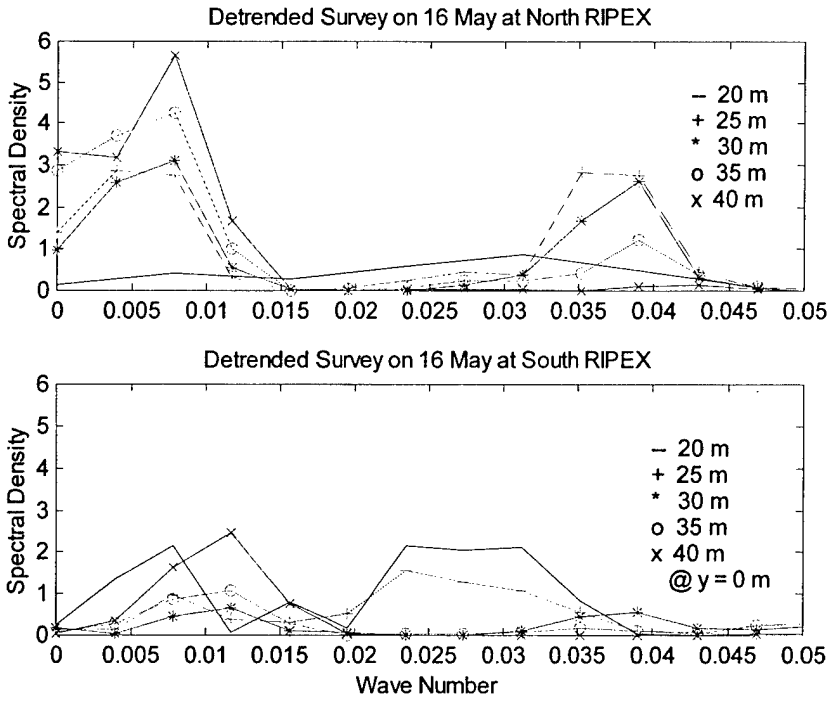

Figure 4-18: Spectral analysis of beach cusp spacing at various cross-shore distances on 16 May

4.1.2 Site 3 & Site 4

A plot of the detrended vertical variation at Site 3 (1000 m ≤ y ≤ 1600 m) on 24 April, corresponding to the longshore transect originating at y = 1000 m, and the corresponding spectral analysis is depicted in Figure 4-19.

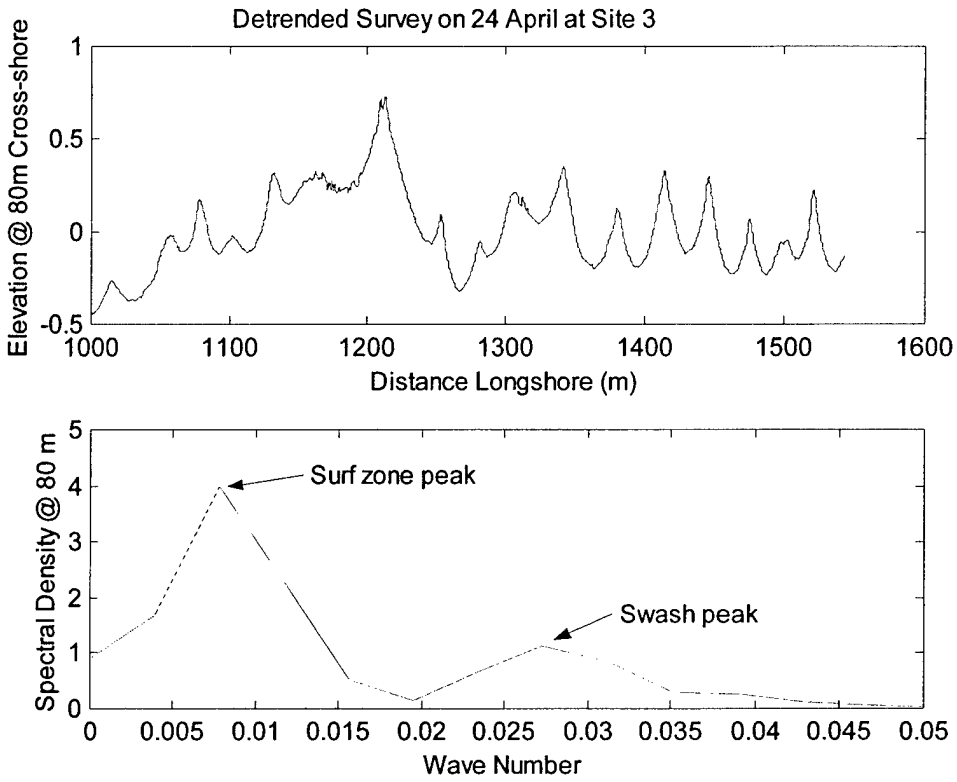

Figure 4-19: Detrended longshore transect at 80 m cross-shore on 24 April at Site 3 and results of spectral analysis showing average surf zone and swash cusp wave numbers

The top plot demonstrates the detrended elevation changes beginning at 80-m cross-shore at a longshore distance of 1000 m. From the bottom plot, the swash cusp peak is at a wave number of 0.0274, or an average cusp wavelength of 36.5 m. Surf zone cusps again demonstrate a strong signal with an average wavelength of approximately 130 m. The results of the spectral analysis performed on survey data from Sites 3 and 4 are summarized for the swash cusps Table 4-2 below.

Table 4-2: Summary of swash cusps at Site 3 and Site 4 from 24 April – 30 April.

Date	Site 3 Primary Spacing	Secondary Spacing	Site 4 Primary Spacing	Secondary Spacing
24 April	36.5 m/42.9 m	N/A	31.9 m	64.5 m
25 April	36.5 m/42.9 m	N/A	36.5 m	52.6 m
26 April	36.5 m/42.9 m	N/A	36. 5 m	N/A
27 April	36.5 m/42.9 m	N/A	36.5 m	52.6 m
29 April	36.5 m/42.9 m	N/A	36.5 m	N/A
30 April	36.5 m/42.9 m	N/A	36.5 m	64.5 m

On 24 April, the primary cusp spacing at Site 3 was the 36.9 m wavelength at 80 m cross-shore, which corresponds to 25 m cross-shore at the North RIPEX site, with a secondary spacing at 42.9 m at 85 m cross-shore. At Site 4, 1600 m $\leq$ y $\leq$ 2200 m, the primary spacing was at a cusp wavelength of 32.2 m at 185 m and 190 m cross-shore, which correspond to 20 m and 25m , respectively, at the North RIPEX site, with a secondary spacing at a 62.4 m wavelength at 190 m, 195 m, and 200 m cross-shore. On 25 April, the spectral energy decreased at Site 3, although the spacing was not significantly affected. However, on this date, the surf zone cusp signal increased and concentrated around the 130 m wavelength at all cross-shore distances. At Site 4, the signal strengths also decreased with a slight shift in the cusp spacing from a peak at 32.2 m to 36.5 m at 185 m cross-shore. The secondary signal at a wavelength of 62.4 m had also been destroyed. The surf zone cusp signal also increased at Site 4 with an average spacing of 130 m at 185 m, 190 m, and 195 m cross-shore.

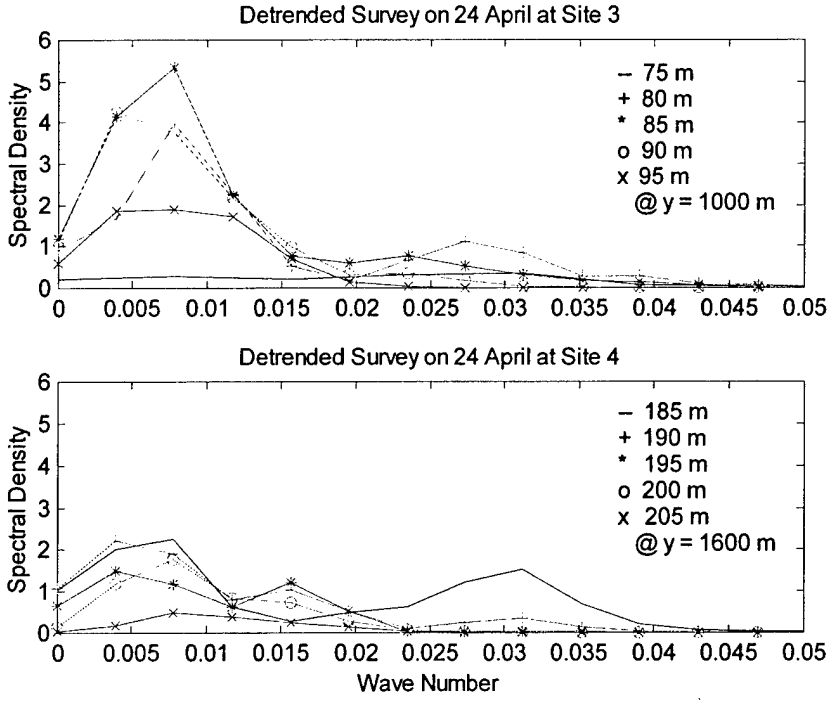

Figure 4-20: Spectral analysis of beach cusp spacing at various cross-shore distances on 24 April

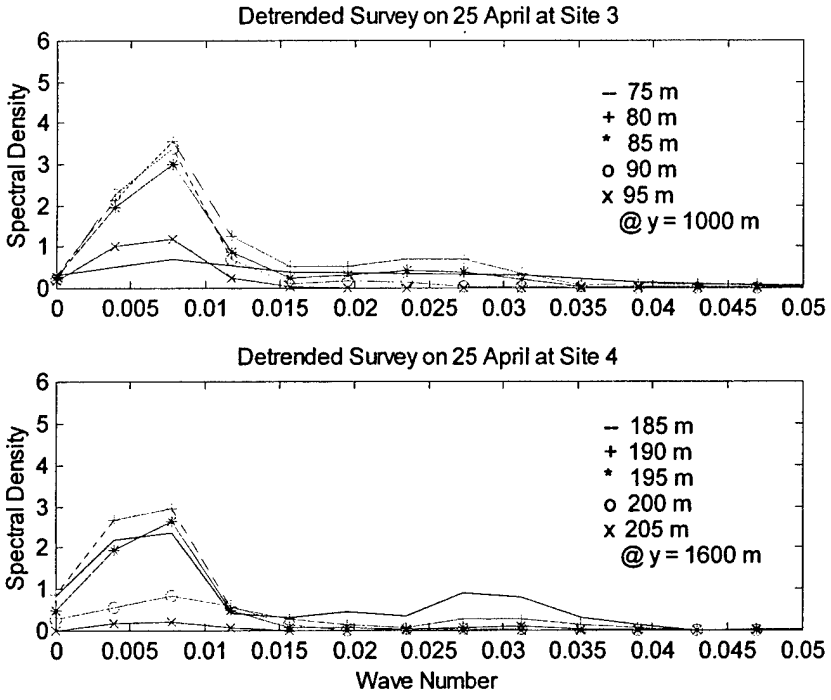

Figure 4-21: Spectral analysis of beach cusp spacing at various cross-shore distances on 25 April

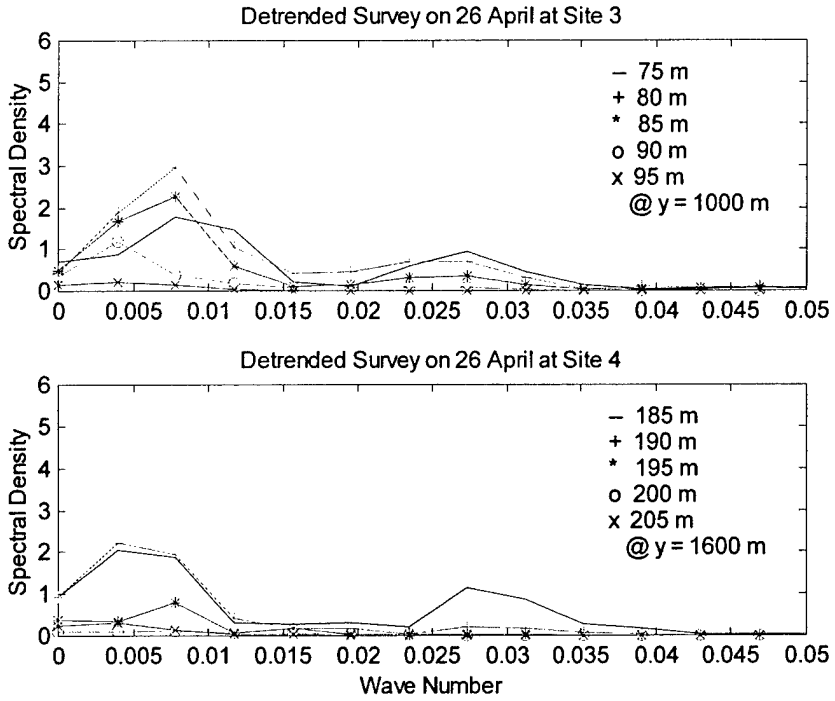

Figure 4-22: Spectral analysis of beach cusp spacing at various cross-shore distances on 26 April

Through 27 April, the signal strength at Site 3 continued to increase around a swash cusp wavelength of 36.5 m at 75 m, 80 m, and 85 m cross-shore. On 29 April, there was a slight shift in wave number energy from the 36.5 m spacing to the 42.6 m spacing at 85 m, 90 m and 95 m cross-shore. This trend continued on 30 April. There was very little change in the spectral energy observed at Site 4 through 27 April. The primary spacing remained at 36.5 m as measured at 185 m cross-shore. However, on 29 April, there was a considerable increase in energy at the 36.5 m wavelength at 185 m, 190 m, and 195 m cross-shore. This trend continued into 30 April with continued increase at this wavelength at 190 m and 195 m cross-shore.

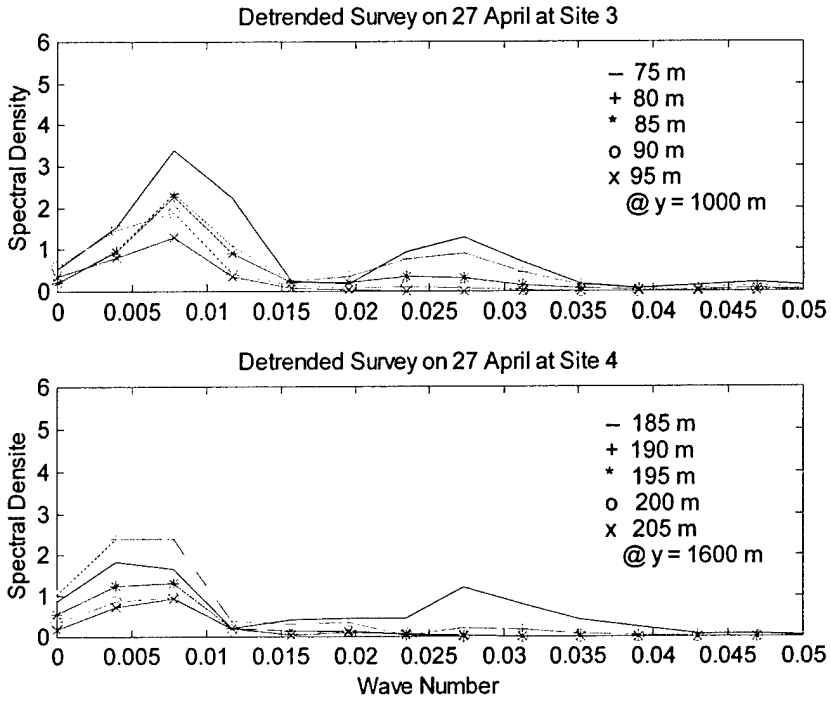

Figure 4-23: Spectral analysis of beach cusp spacing at various cross-shore distances on 27 April

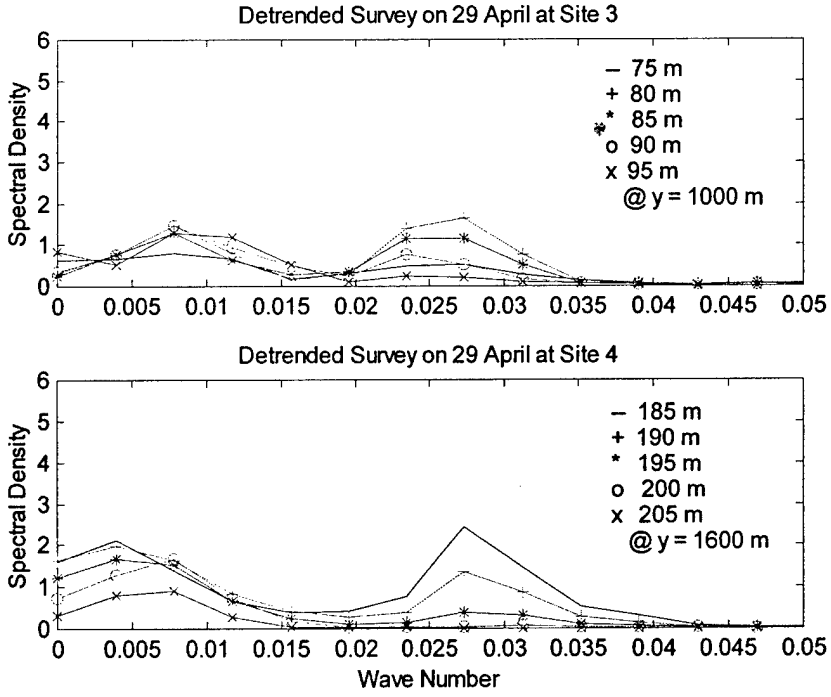

Figure 4-24: Spectral analysis of beach cusp spacing at various cross-distances on 29 April

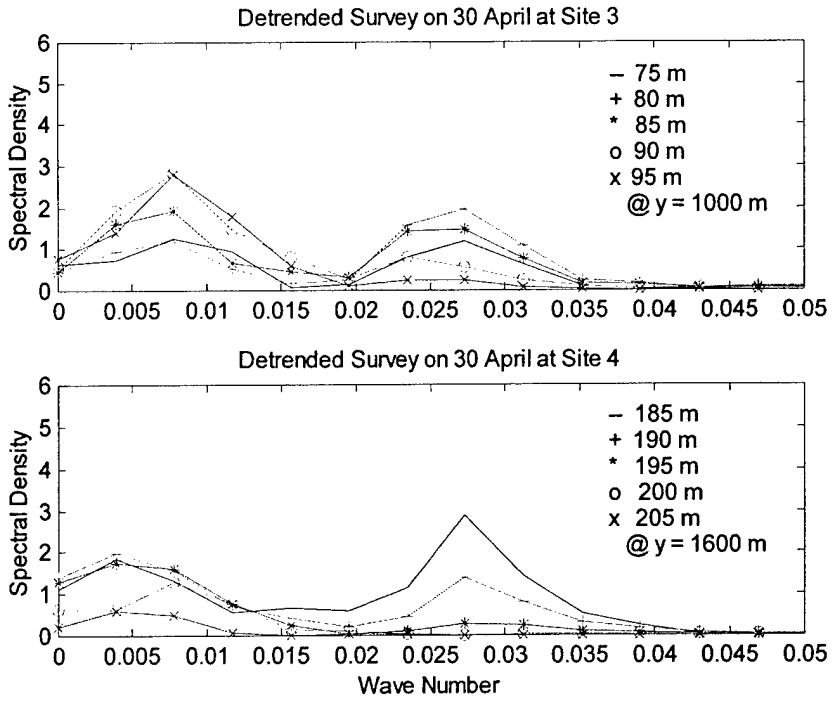

Figure 4-25: Spectral analysis of beach cusp spacing at various cross-shore distances on 30 April

The spectral analyses at these sites show that the average spacing is very stable around the primary average cusp wavelength. There is also very little difference in the primary spacing of all four sites, although all sites have considerably different beach slopes and wave conditions.

Smith (1973) reported that the beach slope varied from 7° – 8° at the northern end of Del Monte Beach to 3° - 4° at the southern end. This information was verified by making cross-shore cuts of the beach at 50 m intervals at each of the four sites. The beach slope was then calculated by determining the elevation change over the near linear portion of the beach slope from the beach slope plot and dividing by the length of run. A sample of the beach slope plots on 30 April for each of the four sites is shown in Figure 4-26 below.

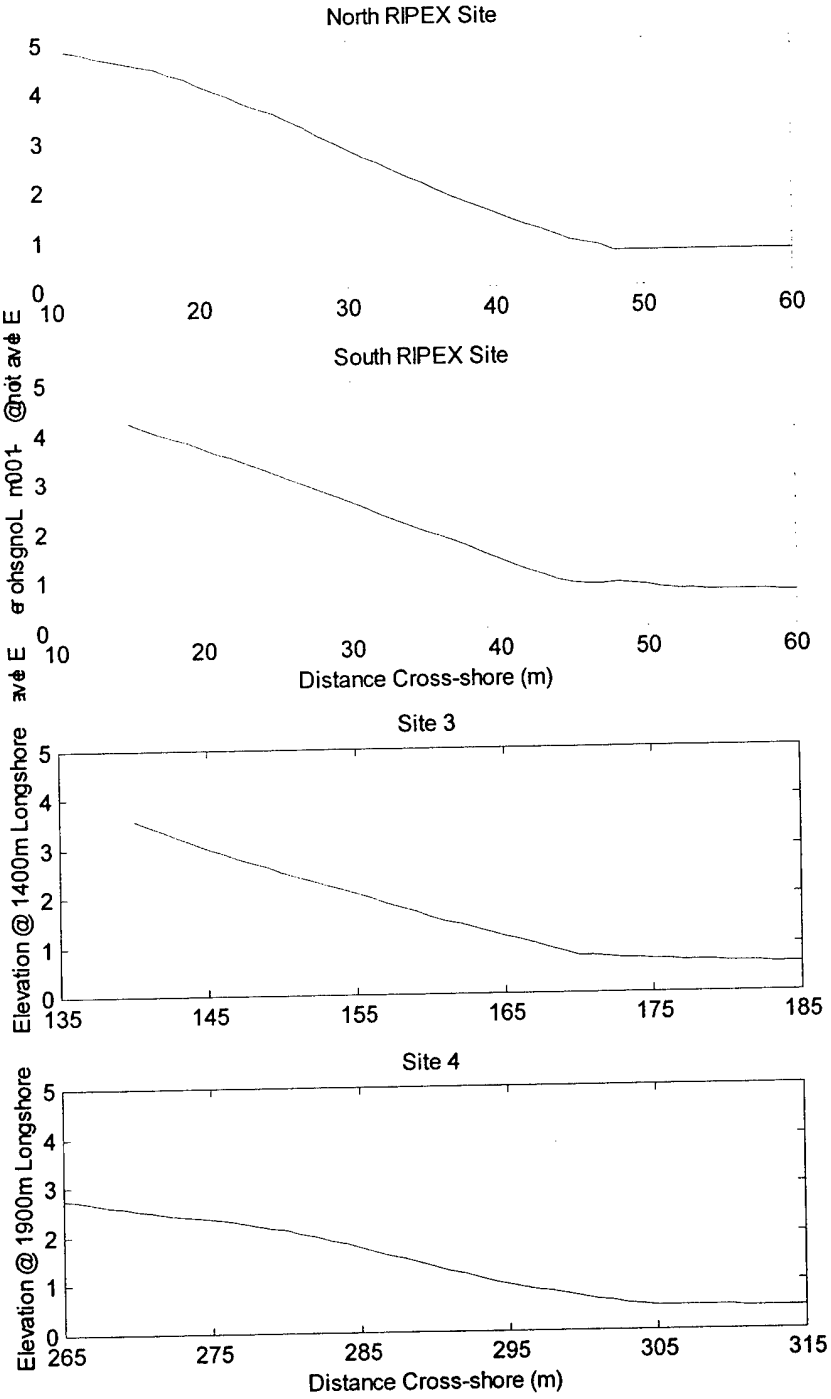

Figure 4-26: Representative beach slopes at each of the four experiment sites on 30 April

These individual slopes were then averaged for each site and survey date to determine the average slope for that site slope for that day. These average site slopes for each survey were compared to determine if there were any significant beach slope changes from survey to survey. There were no significant changes noted during the course of the five-week survey period. The average site slopes for each survey were then averaged again to determine the overall site average for the duration of the data collection. These results are summarized in Table 4-3 below.

Table 4-3: Summary of average beach slope at each experiment site

Experiment Site	Mean Beach Slope	Standard Deviation
North RIPEX	0.131 / 7.5°	0.0111 / 0.64°
South RIPEX	0.109 / 6.2°	0.0164 / 0.94°
Site 3	0.095 / 5.4°	0.0116 / 0.66°
Site 4	0.075 / 4.3°	0.0112 / 0.64°

From this analysis, these results are consistent with those of Smith (1973) with beach slope varying from 7.5° at the north end of Del Monte Beach to 4.3° at the south end of the beach. These calculated slopes for each site were then used in the comparisons of the various beach cusp theories.

4.2 Wave Data Analysis

The nearshore wave period and height were calculated by Jamie MacMahan from the Acoustic Doppler Velocimeter (ADV) raw data collected by the Naval Postgraduate School for the period of 14 April to 21 May. These data are presented in Figure 4-27.

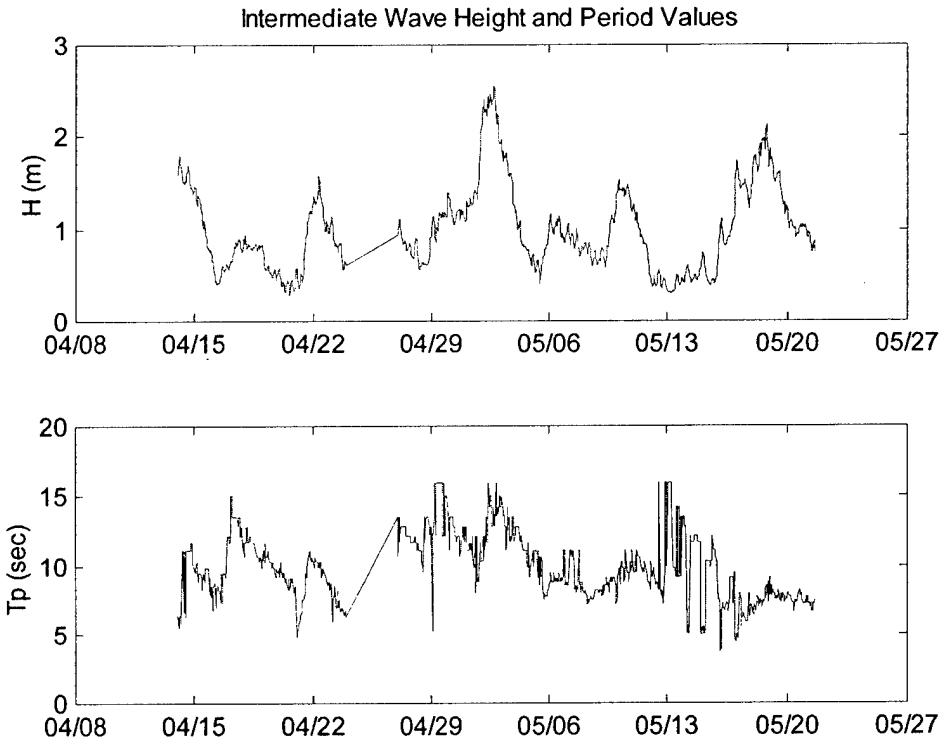

Figure 4-27: Intermediate Wave Height and Period calculated from nearshore ADV

To better apply these wave conditions to prevailing beach cusp theory, an average daily wave period and height were calculated for the period of the RTK-GPS surveys. From these average measured wave conditions, deep water wave height (H_0) and breaking wave height (H_b) were calculated from linear wave theory.

The intermediate wavelength was determined from the wave period and the water depth of the ADV instrument of 6 m. However, the swash cusps observed were formed at high tide, so the average intermediate wavelength was determined using a depth of 7 m, since the average tidal range in this area was 2 m. The wavelength was determined from an iterative process using the linear dispersion relationship:

$$L = (gT^2/2\pi)*\tanh(2\pi h/L) \quad (4.1)$$

Once the intermediate wavelength was calculated, wave number (k) was calculated, which is defined as $2\pi/L$, in order to calculate n and the wave group celerity at the measured conditions. The group celerity was calculated using the following equations:

$$n = 0.5*\{1+[2kh/\sinh(2kh)]\} \quad (4.2)$$

$$C = L/T \text{ and } C_g = nC \quad (4.3)$$

where k is wave number, h is water depth at measured wave conditions, C is wave celerity, and C_g is group celerity. From these calculated average values for each day, the deep water wave height can be determined.

$$H_0 = H\sqrt{[(2C_g)/C_0]} \quad (4.4)$$

where C_0 is deep water wave celerity and defined as L_0/T, and L_0 is defined as $gT^2/2\pi$. The refraction coefficient, K_r, was assumed to be 1.0, since the waves approach the shore at a small angle of incidence. Once H_0 was determined, breaking wave height, H_b was calculated assuming the waves break where $H_b = 0.78h$ (Dean and Dalrymple 1991):

$$H_b = (\kappa/g)^{0.2}(0.5*H_0^2C_0\cos\theta_0)^{0.4} \quad (4.5)$$

where $\kappa = 0.78$ and $\cos\theta_0 \approx 1$. Based on the linear wave theory equations above, the average wave conditions for the period of the experiment are summarized in Table 4-4 below.

Table 4-4: Summary of average wave conditions during experiment

Date	H(avg)	T(avg)	L(avg)	L_0	H_0	H_b	H_0/L_0
14-Apr	1.56	9.23	72.3	133.05	1.54	1.87	0.012
15-Apr	1.07	9.27	72.6	134.13	1.06	1.39	0.008
16-Apr	0.54	9.10	71.1	129.40	0.53	0.80	0.004
17-Apr	0.80	12.77	102.8	254.66	0.70	1.13	0.003
18-Apr	0.79	11.16	89.0	194.38	0.73	1.11	0.004
19-Apr	0.52	10.06	79.5	157.99	0.50	0.79	0.003
20-Apr	0.40	8.13	62.6	103.23	0.41	0.62	0.004
21-Apr	1.00	9.21	72.1	132.47	0.99	1.31	0.007
22-Apr	1.12	8.86	69.0	122.56	1.12	1.43	0.009
23-Apr	0.73	6.90	51.6	74.44	0.77	0.96	0.010
24-Apr	XX	7.00	XX	76.50	0.78	0.97	0.010
25-Apr	XX	10.00	XX	156.13	0.85	1.20	0.005
27-Apr	0.82	12.26	98.5	234.85	0.73	1.16	0.003
28-Apr	0.72	11.80	94.5	217.28	0.65	1.03	0.003
29-Apr	1.13	14.27	115.5	317.94	0.94	1.51	0.003
30-Apr	1.17	12.35	99.2	238.23	1.04	1.54	0.004
1-May	1.42	10.80	85.9	182.10	1.32	1.77	0.007
2-May	2.31	13.05	105.1	265.97	2.00	2.65	0.008
3-May	1.63	13.13	105.9	269.32	1.41	2.01	0.005
4-May	0.84	11.29	90.1	199.04	0.77	1.17	0.004
5-May	0.73	9.28	73.2	134.36	0.72	1.02	0.005

Date	H(avg)	T(avg)	L(avg)	L_0	H_0	H_b	H_0/L_0
6-May	0.99	9.33	73.1	135.79	0.98	1.31	0.007
7-May	0.88	9.30	72.9	135.11	0.86	1.18	0.006
8-May	0.73	7.88	60.3	97.02	0.75	0.99	0.008
9-May	0.99	8.53	66.0	113.54	1.00	1.28	0.009
10-May	1.38	9.71	76.4	147.21	1.34	1.71	0.009
11-May	0.94	9.87	77.8	152.03	0.90	1.26	0.006
12-May	0.42	9.89	78.0	152.66	0.41	0.67	0.003
13-May	0.38	12.39	99.5	239.49	0.34	0.63	0.001
14-May	0.52	9.88	77.9	152.38	0.50	0.79	0.003
15-May	0.56	8.86	69.0	122.49	0.56	0.82	0.005
16-May	1.13	6.85	51.0	73.29	1.20	1.37	0.016

On 24 – 26 April, the acoustic doppler velocimeter (ADV) did not collect any reliable data. Therefore, deep water wave data for 24 – 25 April were obtained from an offshore directional wave buoy, and thus intermediate wave height and wavelength were not obtained for these dates. During the experiment, increased wave energy ($H_b > 1.5$ m) was experienced on 14 April, 29 April – 3 May, and 10 May. However, the only significant storm event occurred on 2 – 3 May, with breaking wave heights > 2.0 m.

The predicted tidal plots for Monterey Bay for the experiment period were obtained from the National Oceanographic and Atmospheric Administration (NOAA) website, and are shown in Figure 4-28 below.

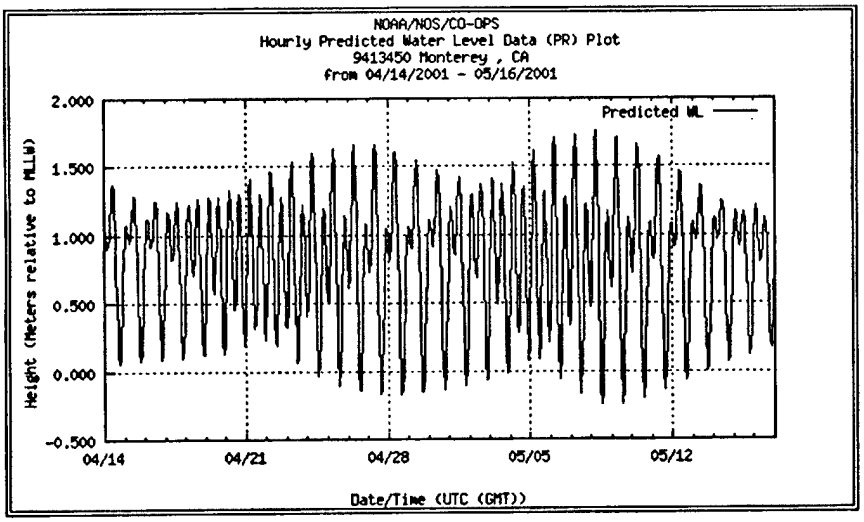

Figure 4-28: Tidal plots for Monterey Bay from 14 April 2001 – 16 May 2001 (NOAA)

The tide is a mixed, predominantly semidiurnal tide, and, from the plot, the maximum observed diurnal inequalities occurred between 28 April – 30 April and 12 May – 14 May. During these times, the water level essentially remains higher for a longer period time, which would allow additional time for cusp formation and maintenance. These dates coincided with periods of observed cusp maintenance, especially during the period of 27 April – 30 April, which was near spring tide.

These variations in wave conditions will be compared with observed variations in the survey data and then compared with prevailing beach cusp theory in an attempt to establish or verify any correlations.

CHAPTER 5
RESULTS AND DISCUSSION

After analysis of the collected survey and wave data, these data were compared to the three primary proposed mechanisms for beach cusp generation and maintenance: edge waves, swash mechanism, and self-organization.

5.1 Edge Wave Mechanism

Edge waves are standing or propagating waves trapped along the shore by refraction. Eckart (1951) developed an equation for relating edge wave longshore wavelength, L_e, and period, T_e, on a planar beach as

$$L_e = (g/2\pi)T_e^2(2n+1)\tan\beta \qquad (5.1)$$

where n is the edge wave mode and β is the beach slope. Based on laboratory experiments and theoretical studies of edge waves and the formation of beach cusps, Guza and Inman (1975) determined that the most easily excited edge wave node is a zero-mode with a period of twice the incident wave period (T_i), and concluded that swash cusp wavelengths are set up by subharmonic edge waves creating longshore periodic perturbations on an initially planar beach. This subharmonic edge wave was hypothesized to result in a cusp wavelength of one-half the edge wavelength:

$$\lambda_c = (g/\pi)\, T_i^2 \tan\beta \qquad (5.2)$$

This proposed spacing was compared to the observed cusp spacing at the experiment site to determine any correlation for the edge wave mechanism.

The incident wave periods and cusp spacing observed for the North and South RIPEX sites are summarized in the following table. As discussed in the Chapter 4, the beach slopes for these sites were determined as 0.131 (for the North RIPEX site) and 0.109 (for the South RIPEX site). From these data, the predicted spacing consistent with edge wave forcing was calculated.

Table 5-1: Comparison of predicted edge wave cusp spacing and observed spacing

Date	Incident Wave Period (T_i)	North RIPEX Predicted Spacing (m)	Observed Spacing (m)	South RIPEX Predicted Spacing (m)	Observed Spacing (m)
14-Apr	9.23	35.06	36.5	29.12	42.9/36.5
15-Apr	9.27	35.34		29.36	
16-Apr	9.10	34.10		28.32	
17-Apr	12.77	67.10		55.74	
18-Apr	11.16	51.22	36.5	42.54	36.5/42.9
19-Apr	10.06	41.63		34.58	
20-Apr	8.13	27.20		22.59	
21-Apr	9.21	34.91		28.99	
22-Apr	8.86	32.29		26.82	
23-Apr	6.90	19.61	36.5	16.29	36.5/42.9
24-Apr	7.00	20.16	36.5	16.74	36.5/42.9
25-Apr	10.00	41.14	42.9/31.1	34.17	42.9/36.5
27-Apr	12.26	61.88	36.5/42.9	51.40	42.9/36.5
28-Apr	11.80	57.25		47.56	
29-Apr	14.27	83.78	36.5/42.9	69.59	42.9/36.5
30-Apr	12.35	62.78	36.5/42.9	52.14	42.9/36.5
1-May	10.80	47.98		39.86	
2-May	13.05	70.09		58.21	
3-May	13.13	70.97		58.95	
4-May	11.29	52.45		43.56	
5-May	9.28	35.40	36.9/28.6/ 21.2	29.41	64.1
6-May	9.33	35.78		29.72	
7-May	9.30	35.60		29.57	
8-May	7.88	25.57	25.6/28.6	21.23	42.9
9-May	8.53	29.92		24.85	
10-May	9.71	38.79		32.22	
11-May	9.87	40.06		33.27	
12-May	9.89	40.23		33.41	
13-May	12.39	63.11	28.6/25.6	52.42	42.9
14-May	9.88	40.15		33.35	
15-May	8.86	32.28		26.81	
16-May	6.85	19.31	25.6/28.6	16.04	42.9

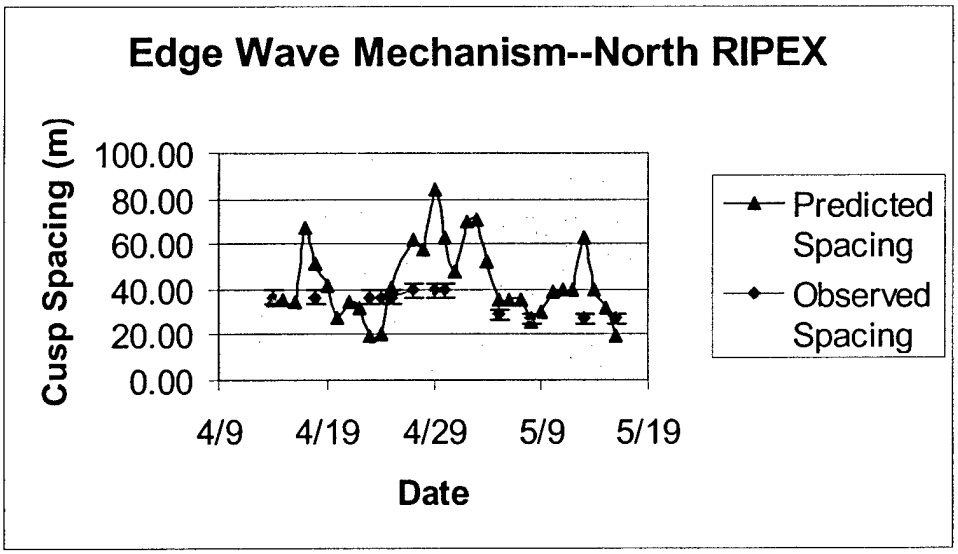

Figure 5-1: Comparison of predicted cusp spacing from edge wave mechanism and observed spacing at the North RIPEX site. The error bars around the observed data represent the error from the discrete bins of the wave number spectrum.

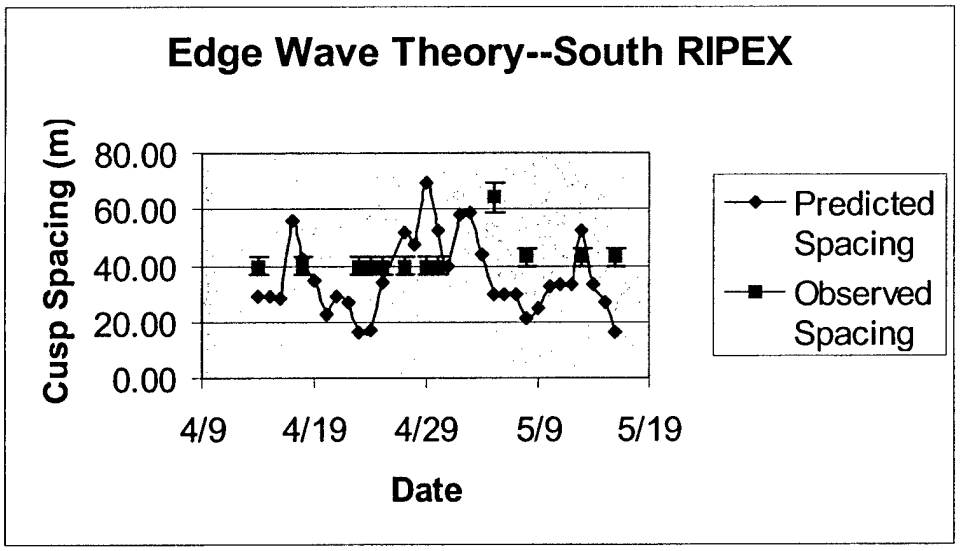

Figure 5-2: Comparison of predicted cusp spacing from edge wave mechanism and observed spacing at the South RIPEX site. The error bars around the observed data represent the error from the discrete bins of the wave number spectrum.

Plots of the predicted cusp spacing from edge wave mechanism and the observed spacing at the North and South RIPEX sites are plotted from the tabular data in Figures 5-1 and 5-2. As witnessed from the plots, there seems to be very little correlation between predicted edge wave spacing due to the instantaneous conditions and the observed spacing at the same time. Since the edge wave equation is a function of the incident wave period, the predicted spacing varies widely due to this dependence. From the observed data, cusp spacing was essentially constant until a storm event on 1 – 2 May destroyed the previous system and allowed a new system of cusps to form with decreased spacing at the North RIPEX site and increased cusp spacing at the South RIPEX site.

Inman and Guza (1973) also related cusp steepness (η_c / λ_c) and beach slope to give upper and lower limits for cusp amplitudes based on the assumption that edge wave activity initiates cusp formation by the following equation:

$$0.13 \leq (\eta_c / \lambda_c \tan\beta) \leq 0.25 \qquad (5.3)$$

where η_c is cusp amplitude, defined as the distance from apex to valley elevation, λ_c is cusp wavelength, and $\tan\beta$ is beachface gradient. This relation for cusp amplitude was compared to the observed cusp amplitude with the same beach slope used in each case. The observed amplitude was calculated by taking the mean differences of the apex and the valley of the cusps from the plots of longshore variation of elevation at each site. The cross-shore distance was selected by using the plot with the strongest spectral signal at the primary cusp wavelength. The results for each of the survey dates are summarized in Table 5-2 below.

Table 5-2: Comparison of predicted cusp amplitude range from the edge wave mechanism and observed amplitude at North and South RIPEX sites.

Date	North RIPEX Predicted Amplitude Range	Observed Mean Amplitude	South RIPEX Predicted Amplitude Range	Observed Mean Amplitude
14 April	0.6 m – 1.15 m	0.50 m	0.41 m – 0.80 m	0.56 m
18 April	0.88 m – 1.69 m	0.43 m	0.61 m – 1.16 m	0.47 m
23 April	0.34 m – 0.65 m	0.44 m	0.23 m – 0.45 m	0.46 m
24 April	0.35 m – 0.66 m	0.40 m	0.24 m – 0.46 m	0.55 m

25 April	0.70 m – 1.36 m	0.48 m	0.49 m – 0.93 m	0.56 m
27 April	1.06 m – 2.04 m	0.45 m	0.73 m – 1.41 m	0.59 m
29 April	1.43 m – 2.76 m	0.40 m	0.99 m – 1.90 m	0.68 m
30 April	1.08 m – 2.07 m	0.56 m	0.74 m – 1.43 m	0.68 m
5 May	0.61 m – 1.17 m	0.45 m	0.42 m – 0.80 m	0.33 m
8 May	0.44 m – 0.84 m	0.42 m	0.30 m – 0.58 m	0.48 m
13 May	1.08 m – 2.08 m	0.41 m	0.75 m – 1.43 m	0.51 m
16 May	0.33 m – 0.64 m	0.45 m	0.23 m – 0.44 m	0.38 m

Again, the theory predicts a widely varying cusp amplitude due to the dependence on incident wave period of the predicted cusp wavelength. However, the observed amplitudes are relatively constant around the mean amplitudes of 0.49 m and 0.57 m at the North and South RIPEX sites, respectively. The theory also predicts that the greater amplitude should occur at the site with the greater beach slope, which is contrary to the observed cusp amplitudes.

5.2 Swash Mechanism

Dean and Maurmeyer (1980) suggested that the cusp spacing is linearly related to maximum swash excursion, and that the most effective beach cusp development occurs when the wave and swash period are approximately equal. Swash period (T_n) can be approximated by:

$$T_n = \sqrt{[(8(\xi_x)_{max}/g \tan \beta]} \quad (5.4)$$

where $(\xi_x)_{max}$ is the maximum uprush distance of the water particle, and tan β is beach slope gradient. Dean and Maurmeyer conducted extensive field measurements of beach cusps and from these measurements they concluded that larger swash excursions resulted in greater beach cusp spacing and proposed the following relationship for cusp spacing.

$$\lambda_c = 4(\xi_x)_{max}\sqrt{\varepsilon} \quad (5.5)$$

$$\varepsilon = (z_h - z_e)/2x\tan\beta = (z_h - z_e)/(z_h + z_e) \quad (5.6)$$

where ε is the relative vertical relief of the cusps, x is the cross-shore distance where cusp horn and embayment elevations were measured. Both x and z are referenced from the still water line, in the horizontal and vertical, respectively . From their field measurements at Drakes Bay Beach, CA, and Point Reyes Beach, CA, they determined that an average value of ε was 0.16, which

reduced Equation (5.5) to $\lambda_c = 1.6(\xi_x)_{max}$, meaning that cusp wavelength was approximately 1.6 times the maximum swash excursion. Takeda and Sunamara (1983) measured combinations of swash excursion and beach cusp spacing and determined that the mean (ξ/λ_c) ratio was 2.0 with a peak at 1.7.

Because data were not collected on swash excursion at the RIPEX sites, theoretical relationships between wave conditions and swash excursion were investigated in order to compare the swash mechanism for beach cusp formation and maintenance to the observed data. Mase (1989) proposed a relationship for representing runup heights of random waves on gentle, smooth and impermeable slopes as a function of the surf similarity parameter (ξ), proposed by Battjes (1974), and deep water wave height. This relationship is

$$R/H_0 = a\,\xi^b \quad \text{for } 1/30 \le \tan\beta \le 1/5 \text{ and } H_0/L_0 \ge 0.007 \tag{5.7}$$

$$\xi = \tan\beta/[\sqrt{(H_0/L_0)}] \tag{5.8}$$

The coefficients were determined by the least squares method. However, the correlation was only valid for conditions where deep water wave steepnesses were smaller than 0.007 for 1/5 slope and smaller than 0.005 for 1/20 and 1/30 slopes. Mase determined the coefficients for maximum runup (R_{max}) as

$$a = 2.32 \text{ and } b = 0.77$$

The experiment beach profile data meet the requirements specified by Mase with beach slopes between 1/5 and 1/30. However, approximately only 60% of the wave data meets the requirement of wave steepness greater than 0.005 for the beach slope greater than 1/30. However, since no other simple relationship exists to calculate swash run-up height from wave data, all wave data was analyzed using this empirical relationship to calculate run-up. Data that do not strictly meet the proposed wave steepness criteria are marked with an asterisk (*). Maximum swash excursion was calculated by the following equation.

$$(\xi_x)_{max} = R_{max}/\tan\beta \tag{5.9}$$

Table 5-3 summarizes the calculations for swash run-up. Swash run-up and excursion are measured in meters.

Table 5-3: Swash run-up and maximum excursion values calculated at the North and South RIPEX sites

Date	Wave Steepness (H_0/L_0)	North RIPEX Maximum Run-up	Swash Excursion	South RIPEX Maximum Run-up	Swash Excursion
14 April	0.012	4.17	31.85	3.62	33.18
15 April	0.008	3.32	25.35	2.88	26.41
16 April	0.004*	2.15*	16.40*	1.86*	17.08*
17 April	0.003*	3.29*	25.13*	2.85*	26.18*
18 April	0.004*	3.06*	23.32*	2.65*	24.29*
19 April	0.003*	2.23*	17.03*	1.93*	17.74*
20 April	0.004*	1.69*	12.90*	1.46*	13.44*
21 April	0.007	3.17	24.22	2.75	25.23
22 April	0.009	3.33	25.41	2.88	26.47
23 April	0.010	2.19	16.70	1.90	17.40
24 April	0.010	2.22	16.95	1.93	17.66
25 April	0.005	3.08	23.52	2.67	24.51
27 April	0.003*	3.29*	25.09*	2.85*	26.14*
28 April	0.003*	2.96*	22.59*	2.57*	23.54*
29 April	0.003*	4.32*	33.00*	3.75*	34.38*
30 April	0.004*	4.10*	31.32*	3.56*	32.63*
1 May	0.007	4.29	32.72	3.72	34.09
2 May	0.008	6.40	48.82	5.54	50.86
3 May	0.005	5.18	39.54	4.49	41.19
4 May	0.004*	3.19*	24.34*	2.76*	25.36*
5 May	0.005	2.63	20.07	2.28	20.91
6 May	0.007	3.18	24.29	2.76	25.30
7 May	0.006	2.94	22.42	2.55	23.36
8 May	0.008	2.38	18.17	2.06	18.93
9 May	0.009	3.01	22.96	2.61	23.92
10 May	0.009	3.99	30.43	3.45	31.70
11 May	0.006	3.17	24.16	2.74	25.17
12 May	0.003*	1.95*	14.87*	1.69*	15.49*
13 May	0.001*	2.06*	15.73*	1.79*	16.39*
14 May	0.003*	2.21*	16.89*	1.92*	17.59
15 May	0.005	2.18	16.61	1.89	17.30
16 May	0.016	2.85	21.77	2.47	22.68

Note: Values with (*) do not meet Mase's condition of wave steepness ≥ 0.005.

The relative vertical relief of the cusps, ε, was calculated similarly to cusp amplitude. The mean differences of the apex and the valley of the cusps from the plots of longshore variation of elevation at each site were divided by the sum of the elevation at the horn and the embayment

at the cross-shore distance with the strongest spectral signal at the primary cusp wavelength (Equation 5.6). These values are summarized in the table below.

Table 5-4: Relative vertical relief values at North and South RIPEX sites

Date	Relative Vertical Relief North RIPEX	Relative Vertical Relief South RIPEX
14 April	0.0742	0.0886
18 April	0.0631	0.0748
23 April	0.0641	0.0724
24 April	0.0582	0.0896
25 April	0.0687	0.0894
27 April	0.0793	0.0937
29 April	0.0731	0.1038
30 April	0.0955	0.1053
5 May	0.0794	0.0609
8 May	0.0765	0.0834
13 May	0.0727	0.0838
16 May	0.0781	0.0633
Average	**0.0733**	**0.0849**

From these values, the average relative vertical relief values at the North and South RIPEX sites were calculated to be 0.0733 and 0.0849, respectively. The average relative vertical relief values and the theoretical swash excursions were then used to calculate the predicted cusp spacing at each site from Equation 5.5. These predicted spacings and the observed spacing are summarized in Table 5-5 below.

Table 5-5: Summary of predicted spacing from swash mechanism and observed spacing at North and South RIPEX sites.

	North RIPEX			South RIPEX		
Date	Max Swash $(\xi_x)_{max}$	Predicted Spacing (λ_c)	Observed Spacing (λ_c)	Max Swash $(\xi_x)_{max}$	Predicted Spacing (λ_c)	Observed Spacing (λ_c)
14 April	31.85	34.5	36.5	33.18	35.9	42.9/36.5
15 April	25.35	27.5		26.41	28.6	
16 April	16.40*	17.8		17.08*	18.5	
17 April	25.13*	27.2		26.18*	28.3	
18 April	23.32*	25.3	36.5	24.29*	26.3	36.5/42.9
19 April	17.03*	18.4		17.74*	19.2	
20 April	12.90*	14.0		13.44*	14.6	
21 April	24.22	26.2		25.23	27.3	
22 April	25.41	27.5		26.47	28.7	
23 April	16.70	18.1	36.5	17.40	18.8	36.5/42.9

24 April	16.95	18.4	36.5	17.66	19.1	36.5/42.9
25 April	23.52	25.5	42.9/31.1	24.51	26.5	42.9/36.5
27 April	25.09*	27.2	36.5/42.9	26.14*	28.3	42.9/36.5
28 April	22.59*	24.5		23.54*	25.5	
29 April	33.00*	35.7	36.5/42.9	34.38*	37.2	42.9/36.5
30 April	31.32*	33.9	36.5/42.9	32.63*	35.3	42.9/36.5
1 May	32.72	35.4		34.09	36.9	
2 May	48.82	52.9		50.86	55.1	
3 May	39.54	42.8		41.19	44.6	
4 May	24.34*	26.4		25.36*	27.5	
5 May	20.07	21.7	36.9/28.6/ 21.2	20.91	22.6	64.1
6 May	24.29	26.3		25.30	27.4	
7 May	22.42	24.3		23.36	25.3	
8 May	18.17	19.7	25.6/28.6	18.93	20.5	42.9
9 May	22.96	24.9		23.92	25.9	
10 May	30.43	32.9		31.70	34.3	
11 May	24.16	26.2		25.17	27.3	
12 May	14.87*	16.1		15.49*	16.8	
13 May	15.73*	17.0	28.6/25.6	16.39*	17.7	42.9
14 May	16.89*	18.3		17.59	19.0	
15 May	16.61	18.0		17.30	18.7	
16 May	21.77	23.6	25.6/28.6	22.68	24.6	42.9

The predicted spacing corresponds reasonably well with the observed spacing on 14 April at both the North and South RIPEX sites. However, once this cusp spacing was "established" on 14 April or perhaps prior to this date, it remained essentially stable until destroyed in the beginning of May, although the predicted spacing varied significantly at both sites. On 2 – 3 May, a storm produced theoretical swash excursions at the sites of approximately 50 m with a predicted cusp spacing of approximately 54 m. This event likely destroyed the cusp system in place since 14 April. The spacing on 5 May remained unstable at both sites. The survey on 8 May demonstrated a new cusp system forming around the 25.6 m/28.6 m at the North RIPEX site and around 42.9 m spacing at the South RIPEX site. The predicted cusp spacing on 6 – 7 May, 26.3 m and 24.3 m respectively, showed a reasonable relation to the observed spacing on 8 May at the North RIPEX site. However, almost nothing in the predicted spacing at the South RIPEX site reasonably correlates with the observed spacing of 42.9 m.

Dean and Maurmeyer also stated that the most effective beach cusp development occurred when the wave and swash period are nearly equal. The swash period was calculated using equation (5.4) and the theoretical maximum swash excursions. A summary of these results is presented in the table below.

Table 5-6: Comparison of calculated swash period at the North and South RIPEX sites and the observed wave period.

Date	Swash Period (T_n) North RIPEX	Swash Period (T_n) South RIPEX	Observed Wave Period (T_i)	Average % Error
14 April	14.1	13.1	9.23	47.3 %
15 April	12.6	11.7	9.27	30.9 %
16 April	10.1	9.4	9.10	7.2 %
17 April	12.5	11.6	12.77	5.4 %
18 April	12.0	11.2	11.16	4.3 %
19 April	10.3	9.6	10.06	1.2 %
20 April	9.0	8.3	8.13	6.4 %
21 April	12.3	11.4	9.21	28.7 %
22 April	12.6	11.7	8.86	37.0 %
23 April	10.2	9.5	6.90	42.6 %
24 April	10.3	9.6	7.00	41.7 %
25 April	12.1	11.3	10.00	16.8 %
27 April	12.5	11.6	12.26	1.6 %
28 April	11.9	11.0	11.80	2.9 %
29 April	14.3	13.3	14.27	3.0 %
30 April	14.0	13.0	12.35	9.1 %
1 May	14.3	13.3	10.80	27.6 %
2 May	17.4	16.2	13.05	29.0 %
3 May	15.7	14.6	13.13	15.3 %
4 May	12.3	11.5	11.29	5.3 %
5 May	11.2	10.4	9.28	16.3 %
6 May	12.3	11.4	9.33	27.3 %
7 May	11.8	11.0	9.30	22.6 %
8 May	10.6	9.9	7.88	30.3 %
9 May	12.0	11.1	8.53	35.4 %
10 May	13.8	12.8	9.71	36.8 %
11 May	12.3	11.4	9.87	20.0 %
12 May	9.6	9.0	9.89	6.1 %
13 May	9.9	9.2	12.39	22.9 %
14 May	10.3	9.5	9.88	0.2 %
15 May	10.2	9.5	8.86	10.8 %
16 May	11.6	10.8	6.85	64.1 %

To quantitatively compare the swash periods to the incident peak wave period, an average swash period was calculated for the two sites. Since these periods should be nearly equal for cusp development, the percent error between the average theoretical swash period and the observed incident wave period was calculated. When the percent error between the two periods was less than 10%, the periods were considered nearly equivalent and therefore should encourage cusp development according to the swash mechanism theory.

The swash period and peak wave period were equivalent during the period from 16 – 20 April with a percent difference less than 7.2 %. However, during this period, there was no significant strengthening of the cusp spacing signal at either site. During the surveys between 14 April and 18 April, a slight increase in the spectral energy was observed at the 30 m cross-shore cut around the 36.5 m cusp spacing at the North RIPEX site. At the South RIPEX site, there were decreases in spectral energy observed at the 25 m, 30 m, and 35 m cross-shore distances around the 42.9 m/36.9 m spacing. The energy at the 20 m cross-shore distance remained unchanged. Between 18 April and 23 April, there were slight increases in energy at the 30 m distance at both the North and South RIPEX sites, while there was little change at the 20 m and 25 m distances. On 23 – 24 April, there were minor decreases in energy at the 25 m and 30 m cuts at the North RIPEX site. However, there was significant change between 23 – 24 April with decreases in the energy observed at the 20 m, 25 m, and 30 m cross-shore cuts at the South RIPEX site. These dates corresponded to strongly non-equivalent wave and swash periods between 21 – 25 April.

From 27 April – 29 April, the swash periods and incident peak wave periods were equivalent within 3.0%, with less than a 10% difference on 30 April. At the North RIPEX site, the spectral energy increased in the 25 m and 30 m cross-shore cuts and focused around the 36.5 m cusp spacing. There were also slight increases in the energy at the 35 m and 40 m cuts through this period around the 36.5 m spacing. No significant change was observed around 20 m. At the South RIPEX site, the 20 m and 30 m signals increased with the 20 m, 25 m, and 30 m signals

focusing around the 42.9 m/36.5 m cusp spacing. Little change in spectral energy was observed in the 35 m and 40 m cross-shore cuts.

During the period 1 – 16 May, only 3 days were recorded with equivalent swash and peak wave periods, 4 May, 12 May, and 14 May. As discussed previously, a new system of cusps were formed beginning sometime after 5 May at the North RIPEX site around a 25.6 m/28.6 m spacing, and around the 42.9 m spacing at the South RIPEX site. Between 5 – 8 May, an increase in spectral energy at the 25 m, 30 m, and 35 m cross-shore cuts was observed at the North RIPEX site. However, between 8 May – 13 May, the energy at 30 m and 35 m decreased appreciably, although it had returned by 16 May. This increase between 13 – 16 May may correspond to the equivalent wave and swash periods on 14 May. There was little change observed at the 25 m cross-shore cut. At the South RIPEX site, the spectral energy at the 20 m and 25 m cross-shore cuts decreased around the 42.9 m spacing and began to disperse between the 42.9 m and 32.2 m spacings from 8 – 16 May.

This analysis was performed using only the peak wave period (which is compared to the swash period). If the wave periods are narrow-banded, the equivalent peak wave period and swash period would likely be constructive to cusp development and maintenance. However, if the incident wave spectrum is broad-banded, it could produce a destructive effect although the incident peak wave period and swash period is still assumed equivalent. Hence, the shape of the wave frequency spectrum should be assessed in order to completely evaluate the effect of wave period.

5.3 Other Empirical Relationships

Masselink (1997) proposed a relationship for beach cusp development based on Battjes' (1974) surf similarity parameter, using breaking wave height. This relationship for cusp development is listed below:

$$\xi = (\tan \beta)/\sqrt{(H_b/L_0)} > 1.2 \qquad (5.11)$$

After analyzing nine years of video imaging data from Duck, NC, Holland (1998) proposed the following empirical relationship for conditions favorable to beach cusp development as a function of storm presence, reflective wave conditions and normal wave incidence.

$$\cos(3|\alpha_b|)/\varphi \geq 0.16 \tag{5.12}$$

Phi, φ, was defined as the surf scaling parameter and was a function of breaking wave height, and beach slope gradient, and α_b was defined as the incident wave angle at breaking.

$$\varphi = (H_b/2)*\omega^2/(g\tan^2\beta) \tag{5.13}$$

$$\omega = 2\pi/T \tag{5.14}$$

The surf-scaling parameter, φ, is related to Masselink's surf similarity parameter, ξ, by the following relationship:

$$\varphi = \pi/\xi^2 \tag{5.15}$$

At the RIPEX experiment sites, incident wave angle, α_b, was approximately zero degrees, which reduced equation (5.12) to $1/\varphi \geq 0.16$. Table 5-7 is a summary of the calculations of the surf similarity parameter, ξ, and the empirical relationship proposed by Holland.

Table 5-7: Summary of Holland's empirical predictor and Masselink's surf similarity parameter at the North and South RIPEX sites.

	North RIPEX		South RIPEX	
Date	**Surf Similarity Parameter, ξ**	**Holland Empirical Predictor**	**Surf Similarity Parameter, ξ**	**Holland Empirical Predictor**
14 April	1.11	0.39	0.92	0.27
15 April	1.29	0.53	1.08	0.37
16 April	1.68	0.90	1.39	0.62
17 April	1.98	1.24	1.64	0.86
18 April	1.74	0.96	1.45	0.66
19 April	1.87	1.11	1.55	0.76
20 April	1.69	0.91	1.41	0.63
21 April	1.32	0.56	1.10	0.38
22 April	1.22	0.47	1.01	0.33
23 April	1.16	0.43	0.96	0.29
24 April	1.17	0.43	0.97	0.30
25 April	1.50	0.72	1.25	0.49
27 April	1.88	1.12	1.56	0.77
28 April	1.91	1.16	1.59	0.80
29 April	1.91	1.16	1.59	0.80
30 April	1.64	0.86	1.36	0.59

1 May	1.34	0.57	1.11	0.39
2 May	1.32	0.55	1.10	0.38
3 May	1.53	0.74	1.27	0.51
4 May	1.72	0.94	1.43	0.65
5 May	1.51	0.72	1.25	0.50
6 May	1.34	0.57	1.11	0.40
7 May	1.41	0.63	1.17	0.44
8 May	1.30	0.54	1.08	0.37
9 May	1.24	0.49	1.03	0.34
10 May	1.22	0.48	1.01	0.33
11 May	1.45	0.67	1.20	0.46
12 May	1.99	1.26	1.66	0.87
13 May	2.57	2.11	2.14	1.46
14 May	1.83	1.07	1.52	0.74
15 May	1.61	0.82	1.33	0.57
16 May	0.96	0.30	0.80	0.20

After calculating Holland's empirical relationship, it was discovered that at Del Monte Beach the value was always greater, and usually much greater, than 0.16. This would imply that either conditions were always favorable to cusp development, or, more likely, that this empirical "cutoff" perhaps only applies to the conditions observed at Duck, North Carolina.

From Masselink's empirical relationship expressed in Equation (5.11), the surf similarity parameter was greater than 1.2 for the majority of the observed days. However, at the North RIPEX site, the surf similarity parameter threshold was not met on 14 April (1.11), 23 – 24 April (1.16 - 1.17), and 16 May (0.96). Since 14 April and 16 May are the borders of collected data, no comparisons can be made with these dates. On the 23 – 24 April, there were minor decreases in observed spectral energy at the 25 m and 30 m cross-shore distances. Following this period, the surf similarity parameter was well above 1.2 from 27 – 30 April, with values ranging from 1.64 – 1.91. During this period, the spectral energy increased in the 25 m and 30 m with slight increases in energy at the 35 m and 40 m cross-shore cuts around the 36.5 m spacing. However, the surf similarity parameter was also well above 1.2 between 16 – 23 April, but very little change was noted in the spectral energy of the cusps during this period.

At the South RIPEX site, the surf similarity threshold was not met on 14 – 15 April (0.92 - 1.08), 21 – 24 April (0.96 - 1.10), 1 – 2 May (1.10 - 1.11), 6 – 10 May (1.01 – 1.17), and 16 May (0.80). Again, comparisons cannot be made with the data on 14 April and 16 May. From survey data between 23 – 24 April at the South RIPEX site, there were significant decreases in observed spectral energy around the 42.9 m/36.5 m spacing at the 20 m, 25 m, and 30 m cross-shore distances. From survey data collected between 5 – 8 May, there were significant decreases of spectral energy at the 20 m and 25 m cross-shore distances around the 64.1 m spacing and at the 20 m distance around the 42.9 m spacing. There was also a slight decrease at the 25 m cross-shore distance around the 42.9 m wavelength. Following this period, the values were greater than 1.2 until 16 May with a peak of 2.14 on 13 May. Between the surveys of 8 – 13 May, there were increases in spectral energy at the 20 m cross-shore distance around the 32.2 m spacing, at 25 m distance around the spacing of 42.9 m, and at the 30 m distance around the 25.6 m cusp spacing. However, there was also a decrease around the 64.1 m cusp spacing at 20 m cross-shore distance.

After comparing the surf similarity parameter threshold with Holland's empirical predictor, it appears that a value of around 0.50 would be a more realistic threshold for cusp formation on Del Monte Beach, CA, than the 0.16 determined at Duck, NC.

Masselink and Pattiaratchi (1998) stated that the degree of horn divergence swash flow, which Werner and Fink (1993) thought was critical to the formation of beach cusps, was a function of the parameter, $\varepsilon(S/\lambda)^2$, referred to as the swash flow parameter in this report, where S was maximum swash excursion and ε quantified the beach cusp prominence and was defined as:

$$\varepsilon = (\tan \beta_{horn} - \tan \beta_{emb})/(\tan \beta_{horn} + \tan \beta_{emb}) \qquad (5.16)$$

This parameter is similar to Dean and Maurmeyer's relative vertical relief parameter (5.6), and the results were verified to be consistent with the results presented in Table 5.4. According to Masselink and Pattiaratchi, horn divergent flow occurs when $0.015 \leq \varepsilon(S/\lambda)^2 \leq 0.15$. When greater than 0.15, overtopping of the cusp horns occurs and thus the horns are eroded and

accretion occurs in the embayments. Table 5-8 presents a summary of the calculations for this parameter for each survey date using observed primary cusp spacing, the observed relative relief parameter, and the theoretical maximum swash excursion.

Table 5-8: Summary of swash flow parameter results for each survey date

	North RIPEX			South RIPEX		
Date	**Maximum Swash Excursion**	**Observed Primary Cusp Spacing**	**Swash Flow Parameter $\varepsilon(S/\lambda)^2$**	**Maximum Swash Excursion**	**Observed Primary Cusp Spacing**	**Swash Flow Parameter $\varepsilon(S/\lambda)^2$**
14 April	31.85	36.6	0.056	33.18	39.7	0.062
18 April	23.32	36.6	0.026	24.29	39.7	0.028
23 April	16.70	36.6	0.013	17.40	39.7	0.014
24 April	16.95	36.6	0.012	17.66	39.7	0.018
25 April	23.52	36.6	0.028	24.51	39.7	0.034
27 April	25.09	39.7	0.032	26.14	39.7	0.041
29 April	33.00	39.7	0.051	34.38	39.7	0.078
30 April	31.32	39.7	0.059	32.63	39.7	0.071
5 May	20.07	28.9	0.038	25.36	64.1	0.006
8 May	18.17	27.1	0.034	18.93	42.9	0.022
13 May	15.73	27.1	0.024	16.39	42.9	0.012
16 May	21.77	27.1	0.050	21.77	42.9	0.024

The swash flow parameter was calculated below the 0.015 threshold on 23 – 24 April at the North RIPEX site, and on 23 April, 5 May, and 13 May at the South RIPEX site. The 23 – 24 April values correspond to the surf similarity parameter less than 1.2 at the North RIPEX site. However, it is difficult to conclude very much from this information since the surf similarity parameter could only be calculated on survey dates. Also, six of these dates do not meet Mase' criteria for wave steepness when calculating swash excursion. It would have also been interesting to calculate the swash flow parameter during the storm event on 2 – 3 May to verify if it would have exceeded the upper threshold of 0.15 for overtopping of the cusp horns.

CHAPTER 6
SUMMARY AND CONCLUSIONS

From the five weeks of survey data collected from 5 April – 16 May 2001 on Del Monte Beach, CA, the observed swash zone cusp spacing was found to remain remarkably stable at relatively fixed longshore wavelengths until a storm event occurred to destroy that cusp pattern; hence once cusp spacing was established it did not adjust to the existing wave conditions. This pattern supports the observations of Wright et al. that once cusp spacing has been cut into a beach, it will dominate until a wave event occurs that establishes a different cusp spacing. Unfortunately, during the observation period, there was only one storm event significant enough to radically change the beach cusp spacing. Another interesting observation was that the initial cusp spacing remained essentially constant along the entire length of the beach, despite the fact that the beach slope decreased from 7.5° to approximately 4.5° from north to south and that the wave heights at the south end were observed to be approximately half the wave heights at the north end of the experiment site.

When comparing the observed cusp spacing with the predicted spacing resulting from edge wave forcing, the results did not correlate very well. Since the predicted spacing from an edge wave mechanism is a function of incident wave period, the predicted spacing varied widely over the survey period, while the observed spacing did not, as witnessed in Figures 5-1 and 5-2. The edge wave mechanism also predicts increased spacing with increasing beach slope. As noted, the spacing before the storm event on 2 – 3 May was essentially constant around the 36.9 m/42.9 m wavelength along the entire length of beach. The predicted cusp amplitude range also didn't correspond to the observed cusp amplitudes. Again, predicted amplitude was a function of the predicted cusp spacing, and therefore varied significantly from day to day, while the observed amplitudes remained reasonably stable at each separate experiment site. The one possible positive correlation for the edge wave mechanism occurred at the North RIPEX site on 14 April and 8 May. Inman and Guza (1982) proposed that cusp formation begins with an initial rhythmic

disturbance caused by subharmonic edge waves, and then grows under a constructive swash mechanism. On these dates, the predicted spacing coincides with the observed spacing at the North RIPEX site. The 14 April cusp spacing remained fixed until the storm event of 2 – 3 May, and the 8 May spacing remained fixed until the end of the survey period. However, the same mechanism does not adequately explain the cusp spacing at the adjacent South RIPEX site during these same time periods.

The "swash mechanism" predicted spacing was difficult to compare with the observed spacing because the necessary swash excursion data were not recorded during the field experiment. Therefore, an empirical relationship was used to approximate swash excursions from deep water wave heights. There were also problems with this method since the wave steepness criteria for using the empirical coefficients for maximum run-up were not met for all data. However, since no other simple empirical relationships were found relating wave conditions to swash run-up, this relationship was used for all comparisons. The predicted spacing for this mechanism corresponds better with the observed data, but it still does not accurately describe the spacing due to its strong dependence on varying swash excursion. The predicted spacing does correspond fairly well to the observed spacing on the first survey date, and on the two days preceding the 8 May survey at the North RIPEX site. However, there is a suggestion that when the predicted cusp spacing exceeds the observed spacing, as in storm conditions, it may be indicative of a change in the overall beach cusp spacing. From the observed data, the predicted swash zone cusp spacing never exceeded the observed spacing until the storm event on 2 – 3 May; during which time, the previous pattern was destroyed to allow a new pattern to form on the beach.

Comparisons between the theoretical swash period and the observed wave period did provide some evidence for a swash maintenance mechanism. When these periods were nearly equal, cusp development was observed in the spectral analysis. During the period of 27 – 30 April, this was particularly noticeable, with strengthening of the spectral energy around the

primary cusp wavelengths observed at all four experiment sites. During this time the theoretical swash period was calculated to be within 3% of the observed wave period. This was also the best period to observe cusp development and validate this theory. Typically, there were days of equivalent swash/wave periods and non-equivalent days in between the survey data, which made additional validation of this mechanism difficult.

Under the self-organization mechanism, random perturbations on the beachface organize themselves into beach cusps under horn divergent swash flow conditions. It was difficult to make any conclusions on the causative aspects of this theory, since beach cusps were always present during the survey period. There were periods of reduced vertical relief and one period where the cusp spacing was destroyed by a storm event, but the beach was never in a planar state to determine how the cusps first formed. Therefore, this analysis will concentrate only on the development of beach cusps under horn divergent flow conditions and the utility of other predictive indices.

Holland's (1998) empirical predictive index for conditions favorable to cusp formation did not appear to translate well to Del Monte Beach from Duck, NC, where the relationship was developed. The conditions at Del Monte Beach using this index were always favorable to cusp formation. However, considering those times when cusps degraded, and also when comparing Holland's threshold value of 0.16 with the surf similarity parameter proposed by Masselink (1997), it appears that a more appropriate value at the Del Monte Beach might be approximately 0.50 for conditions favorable for cusp development.

Masselink's (1997) threshold involving the surf similarity parameter appears to hold that when the value is less than 1.2, conditions are not conducive to cusp development. This was demonstrated with the data from the South RIPEX site. However, at the North RIPEX site, this threshold was not exceeded on only four days, implying that almost the entire period was conducive to cusp development, which again was contrary to the observed results. This would appear to be a result of the increased beach slope at the North RIPEX site, and the fact that the

linear wave equation used for calculating breaking wave height was independent of beach slope. The conditions for beach cusp development at the South RIPEX site should be similar to the conditions for development at the adjacent North RIPEX site. Under this assumption, the surf similarity threshold for the North RIPEX site should be on the order of 1.45 instead of 1.20.

Analysis of Masselink and Pattiaratchi (1998) swash flow parameter was difficult since this parameter is a function of cusp spacing and maximum swash excursion. Since the daily-predicted cusp spacing was determined from the empirical swash excursions (Equation 5.5), this parameter could only be calculated from the observed cusp spacing and empirical swash excursions. From Table 5.8, there was only one date where the swash flow parameter was less than 0.015, and that was because of a large primary cusp spacing of 64.1 m on 5 May due to an apparently "unstable" cusp system following the 2 – 3 May storm event. There were also no dates recorded where the swash flow parameter was greater than 0.15 (meaning that the swash was overtopping the established horns). It would seem reasonable that this occurred during the storm event on 2 – 3 May, but such conditions are unfortunately not the ideal time to conduct beach surveys. However, if swash excursion data were collected, it would have been interesting to see if there were any other conditions that would have exceeded the 0.15 threshold.

Based on the literature review performed and the data collected, it would be difficult to draw conclusions regarding a causative mechanism for beach cusp development. Edge wave lengths, based on incident wave conditions only, were consistent with the newly developed pattern of cups following the 2 – 3 May storm, but only at the North RIPEX site and not the south. There was also only one definitive cusp formation "event" during the entire experimental record on which to base such analysis. To validate the edge wave mechanism for beach cusp development, one would have to devise a better method of detecting edge wave energy in the surf zone and then relating that energy to the beachface morphology. This theory is further complicated by the fact that it appears that once cusps are formed on the beach, they are a stable feature until radically different wave conditions change them. So to validate the edge wave

mechanism, edge wave energy would have to be recorded during that critical period of cusp change. To validate the self-organization theory, a beach would have to be observed through several cycles from planar beach to cusped beach to determine if there are any relic features that promote cusp development and if the cusps propagate from these features along the beach, or instead form instantaneously along the beach.

However, from the data collected at this site, cusp maintenance conditions can be reasonably explained from the current theories. Cusp development appears to occur under horn divergent flow, as described by the swash flow parameter, and when the swash period is nearly equal, less than 5% difference, to that of the incident waves. When these two conditions are met, conditions are most conducive to cusp development. Cusp destruction occurs under more energetic wave conditions, where the swash excursion is sufficient to sweep over the existing cusp horns. Comparing Dean and Maurmeyer's relation between swash excursion and cusp spacing with the observed data, when the predicted spacing exceeded the observed cusp spacing that cusp system was destroyed. However, since only one storm event was observed, it was inconclusive as to whether this relation accurately predicted the cusp spacing following the storm event.

Since it appears that cusp initiation begins with an initial perturbation and then develops under a swash feedback mechanism, it will always be challenging to record the event that begins the process. However, for follow-on experiments on beach cusps, it is recommend that the experiment take place over a sufficient period of time to observe multiple storm events that have the potential to destroy the existing cusp system. An accurate measure of recording swash excursions and beach changes is recommended through the use of video imaging, with RTK-GPS surveys used for calibrating the video imagery data. A method of measuring edge wave energy in the nearshore is also recommended to further examine edge waves as a causative mechanism.

APPENDIX
ADDITIONAL TOPOGRAPHICAL BEACH SURVEYS

The following plots are additional topographical plots of the North and South RIPEX experiment sites from 18 April 2001 – 16 May 2001.

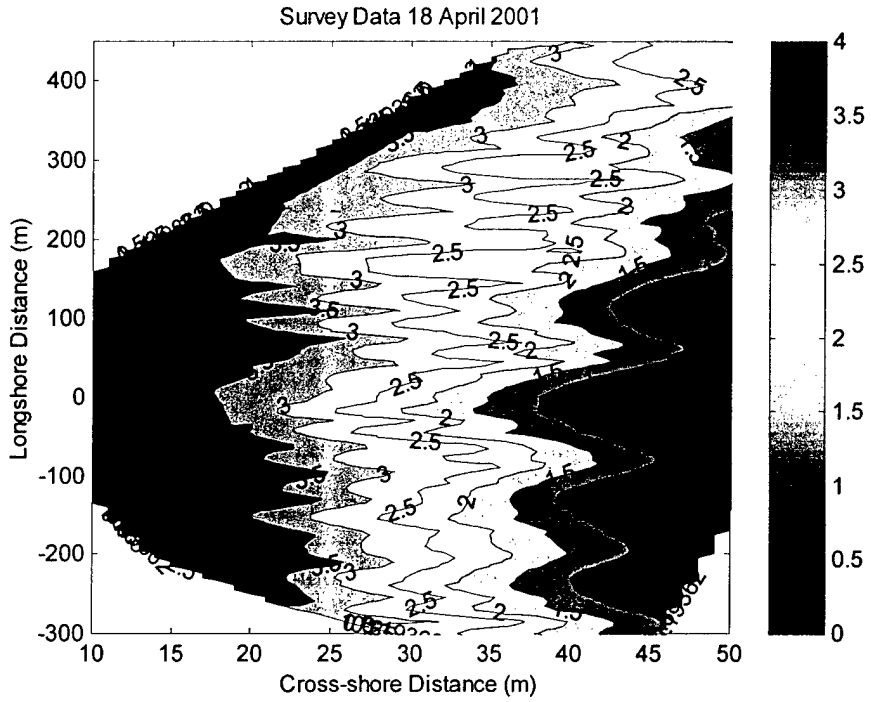

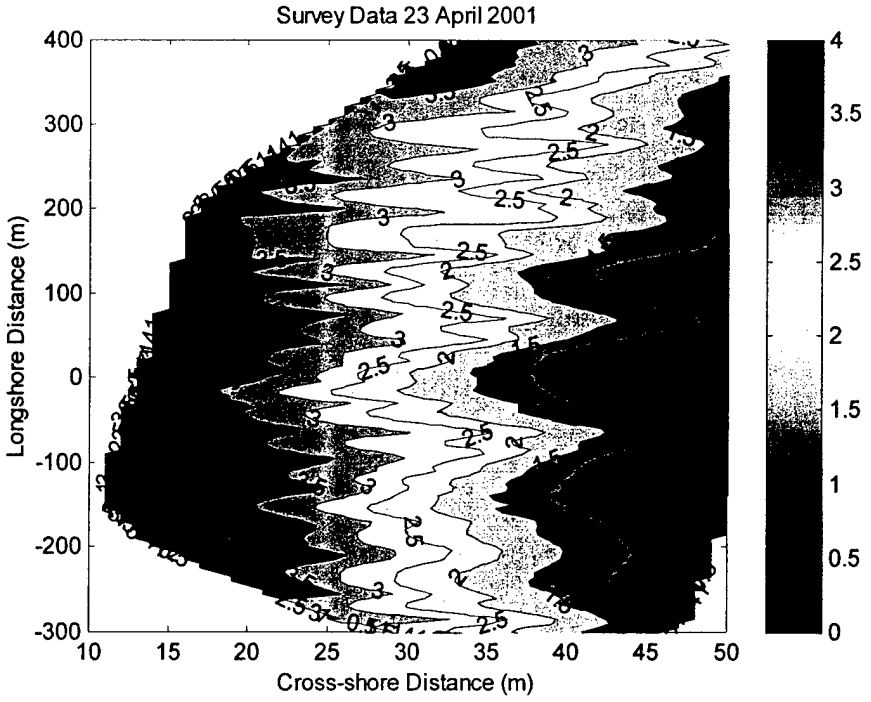

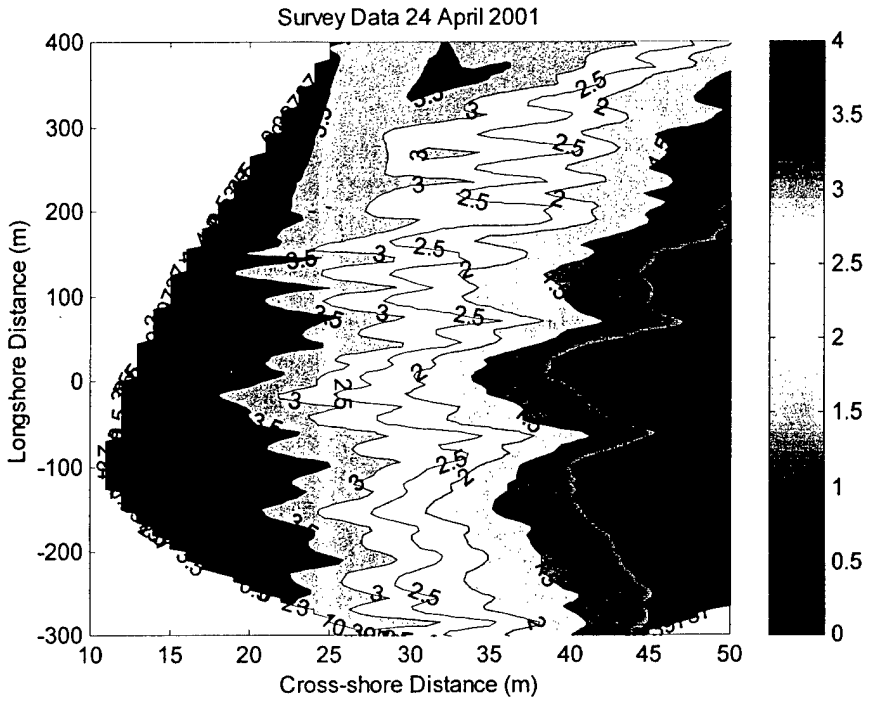
Survey Data 24 April 2001
Longshore Distance (m)
Cross-shore Distance (m)
400
300
200
100
0
-100
-200
-300
10
15
20
25
30
35
40
45
50
4
3.5
3
2.5
2
1.5
1
0.5
0

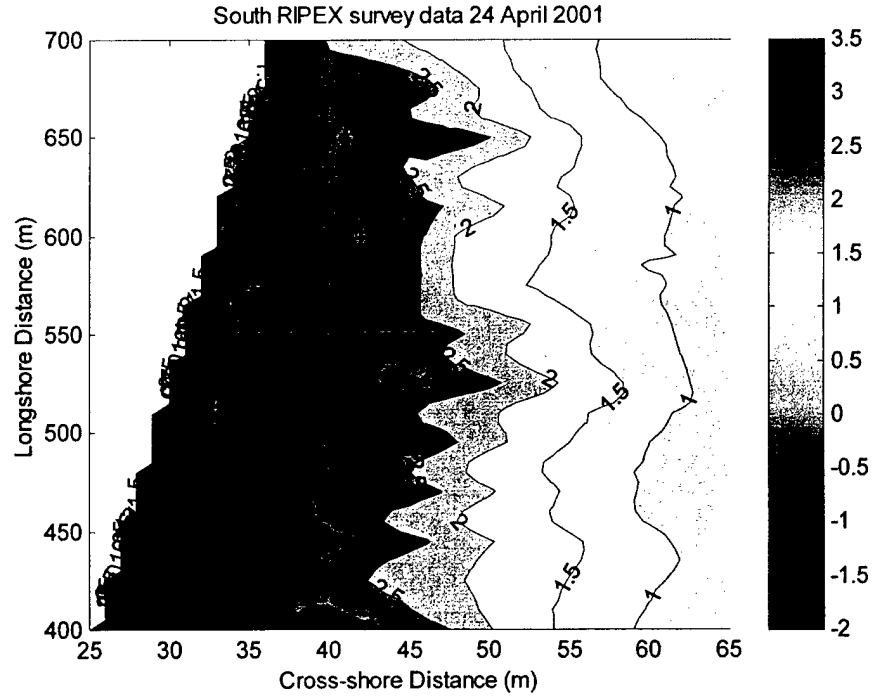
South RIPEX survey data 24 April 2001
Longshore Distance (m)
Cross-shore Distance (m)
700
650
600
550
500
450
400
25
30
35
40
45
50
55
60
65
3.5
3
2.5
2
1.5
1
0.5
0
-0.5
-1
-1.5
-2

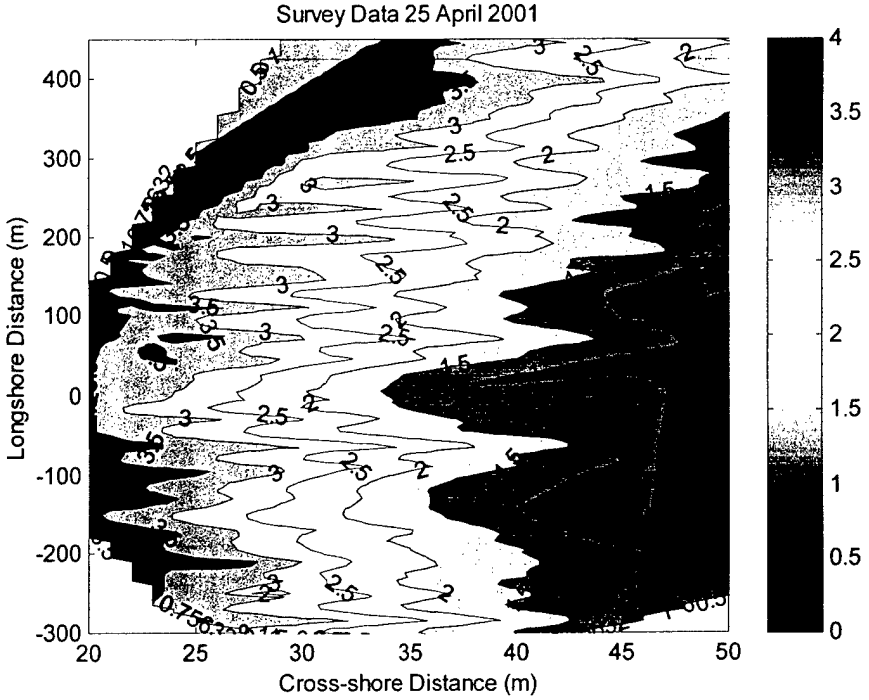
Survey Data 25 April 2001
Longshore Distance (m)
Cross-shore Distance (m)
400
300
200
100
0
-100
-200
-300
20
25
30
35
40
45
50
4
3.5
3
2.5
2
1.5
1
0.5
0

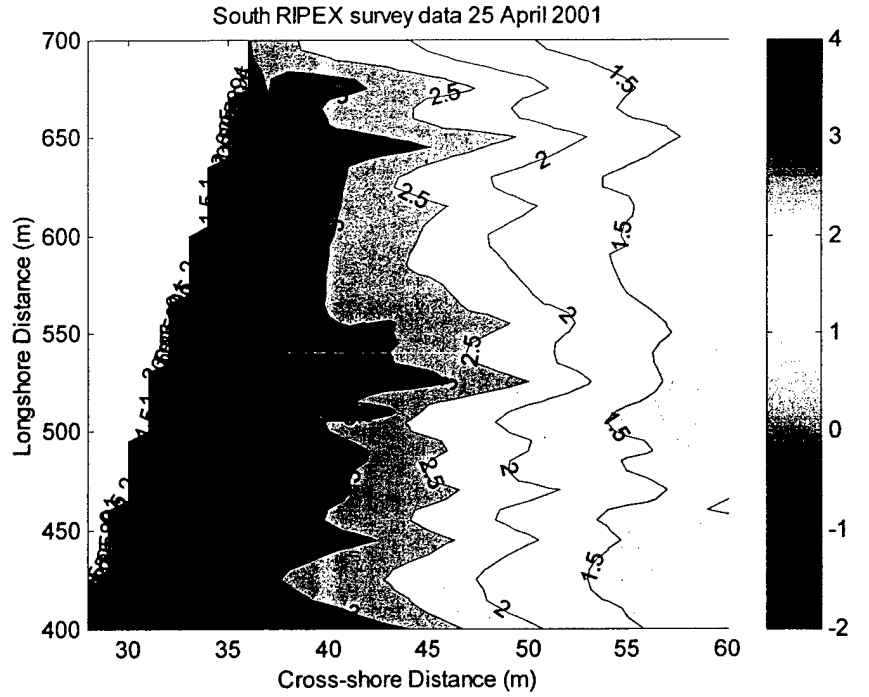
South RIPEX survey data 25 April 2001
Longshore Distance (m)
Cross-shore Distance (m)
700
650
600
550
500
450
400
30
35
40
45
50
55
60
4
3
2
1
0
-1
-2

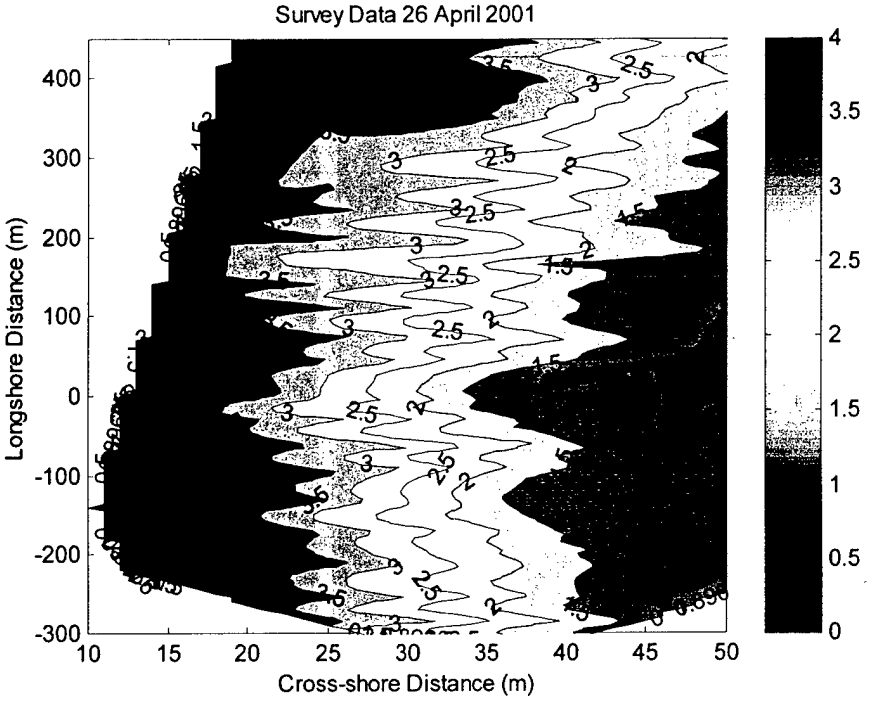
Survey Data 26 April 2001
Longshore Distance (m)
Cross-shore Distance (m)
400
300
200
100
0
-100
-200
-300
10
15
20
25
30
35
40
45
50
4
3.5
3
2.5
2
1.5
1
0.5
0

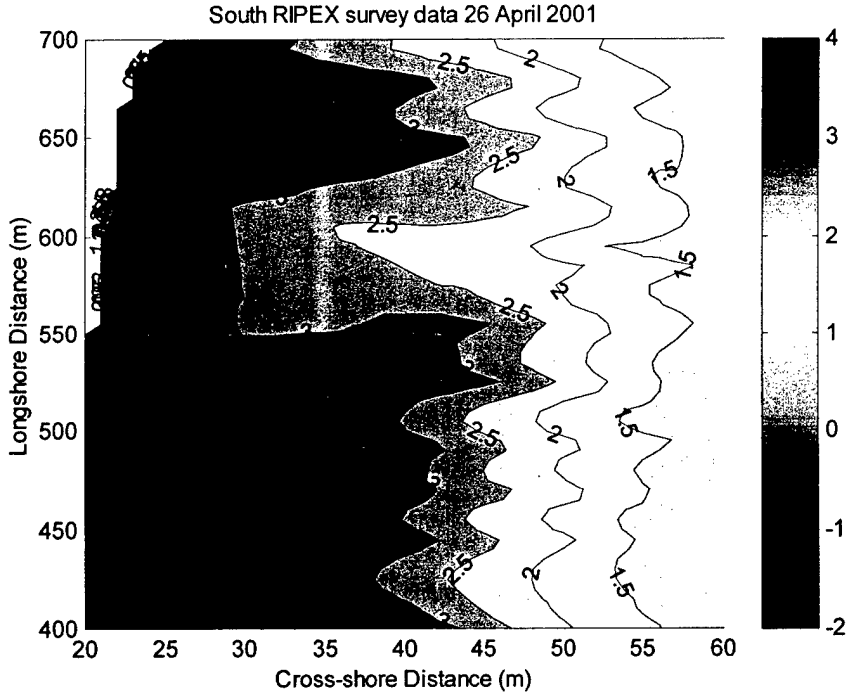
South RIPEX survey data 26 April 2001
Longshore Distance (m)
Cross-shore Distance (m)
700
650
600
550
500
450
400
20
25
30
35
40
45
50
55
60
4
3
2
1
0
-1
-2

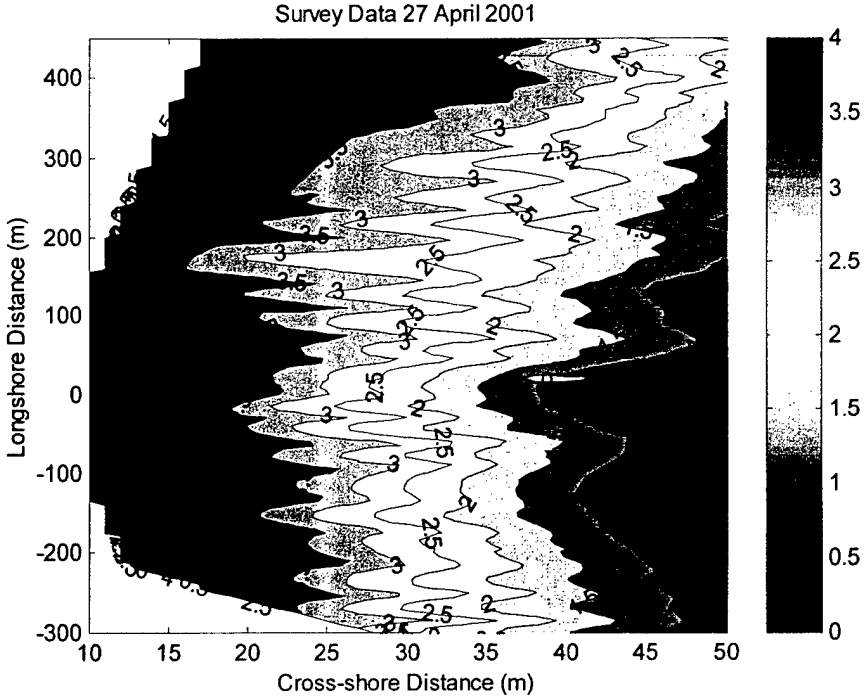
Survey Data 27 April 2001
Longshore Distance (m)
Cross-shore Distance (m)
400
300
200
100
0
-100
-200
-300
10
15
20
25
30
35
40
45
50
4
3.5
3
2.5
2
1.5
1
0.5
0

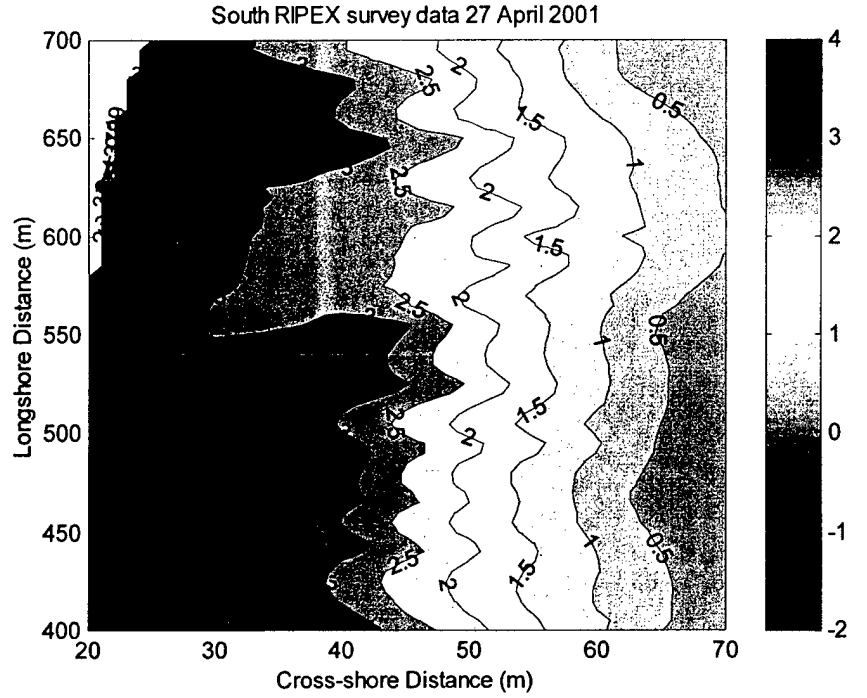
South RIPEX survey data 27 April 2001
Longshore Distance (m)
Cross-shore Distance (m)
700
650
600
550
500
450
400
20
30
40
50
60
70
4
3
2
1
0
-1
-2

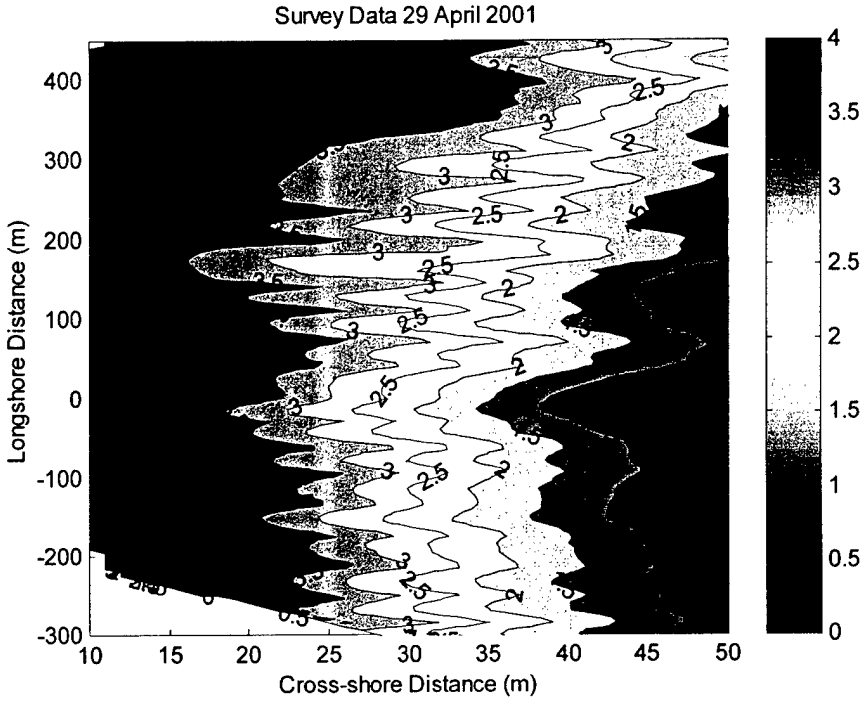
Survey Data 29 April 2001
Longshore Distance (m)
Cross-shore Distance (m)
400
300
200
100
0
-100
-200
-300
10
15
20
25
30
35
40
45
50
4
3.5
3
2.5
2
1.5
1
0.5
0

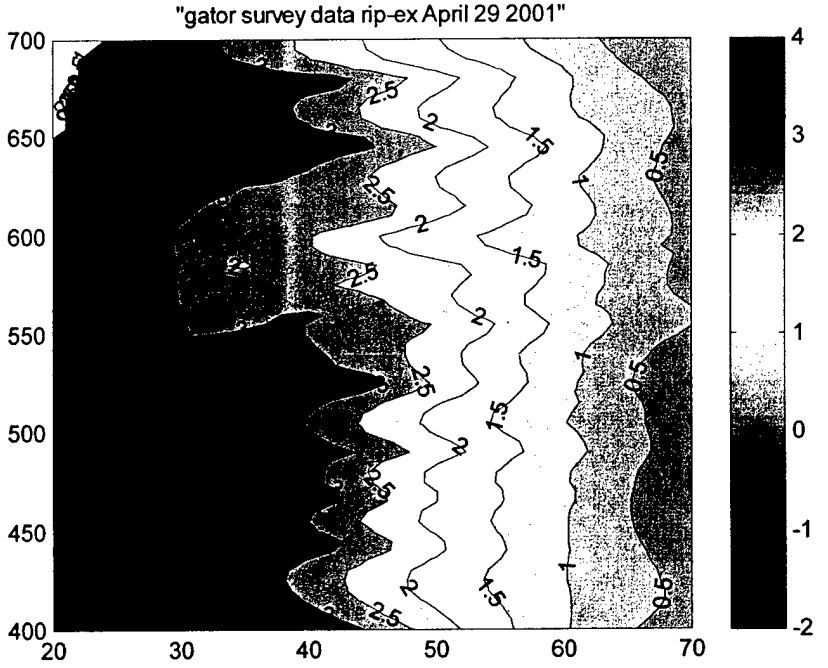
"gator survey data rip-ex April 29 2001"
700
650
600
550
500
450
400
20
30
40
50
60
70
4
3
2
1
0
-1
-2

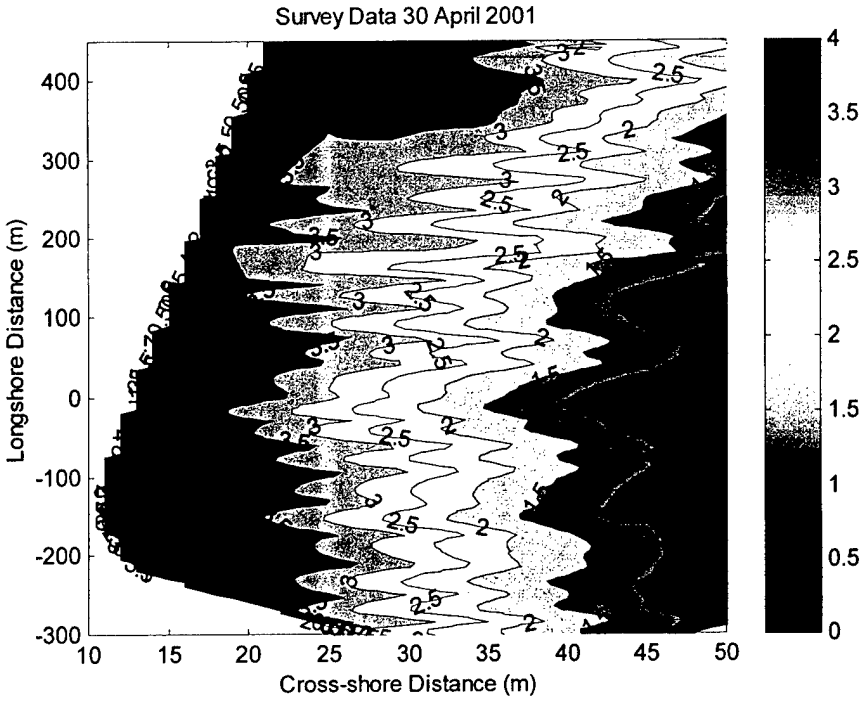
Survey Data 30 April 2001
Longshore Distance (m)
Cross-shore Distance (m)
400
300
200
100
0
-100
-200
-300
10
15
20
25
30
35
40
45
50
4
3.5
3
2.5
2
1.5
1
0.5
0

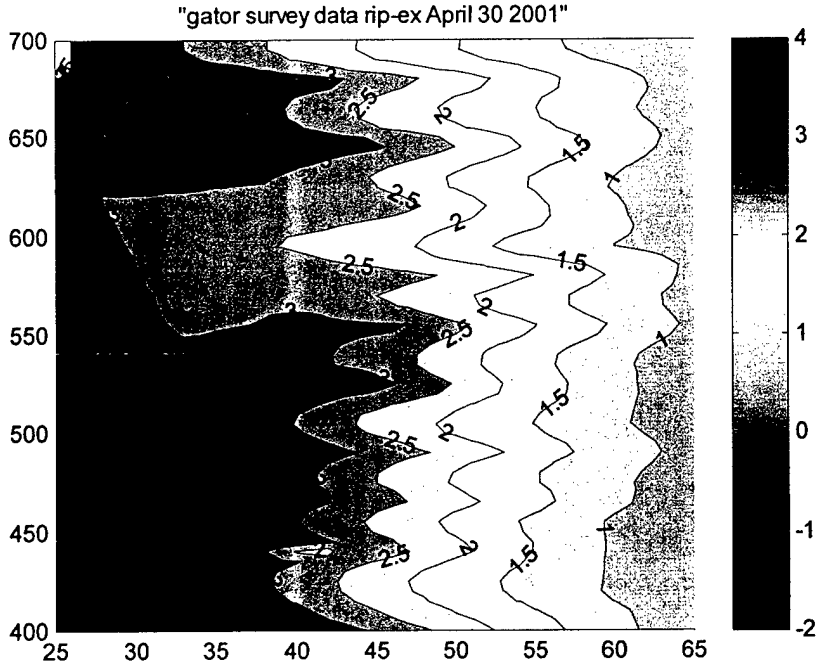
"gator survey data rip-ex April 30 2001"
700
650
600
550
500
450
400
25
30
35
40
45
50
55
60
65
4
3
2
1
0
-1
-2

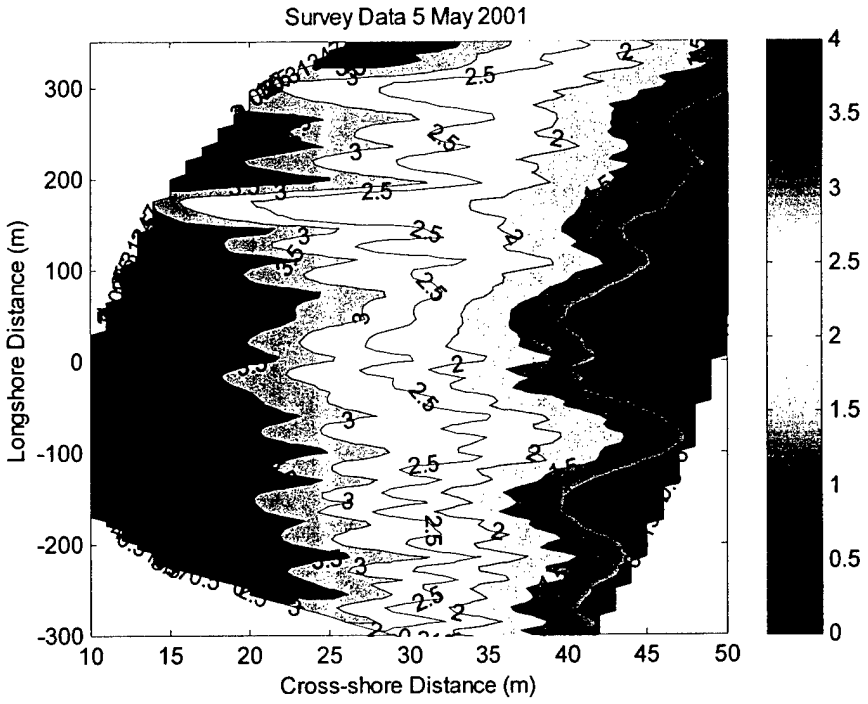
Survey Data 5 May 2001
Longshore Distance (m)
Cross-shore Distance (m)
300
200
100
0
-100
-200
-300
10
15
20
25
30
35
40
45
50
4
3.5
3
2.5
2
1.5
1
0.5
0

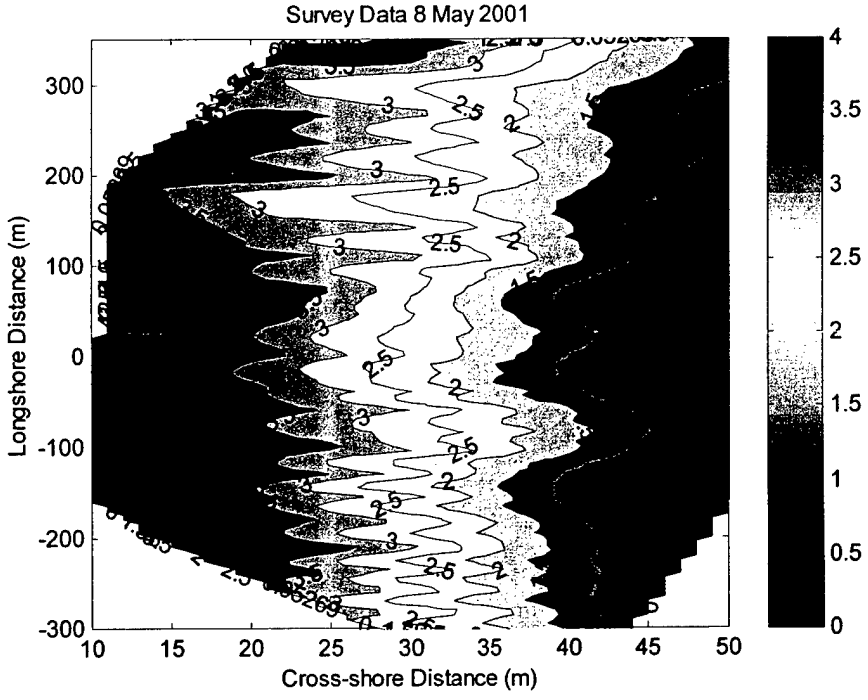
Survey Data 8 May 2001
Longshore Distance (m)
Cross-shore Distance (m)
300
200
100
0
-100
-200
-300
10
15
20
25
30
35
40
45
50
4
3.5
3
2.5
2
1.5
1
0.5
0

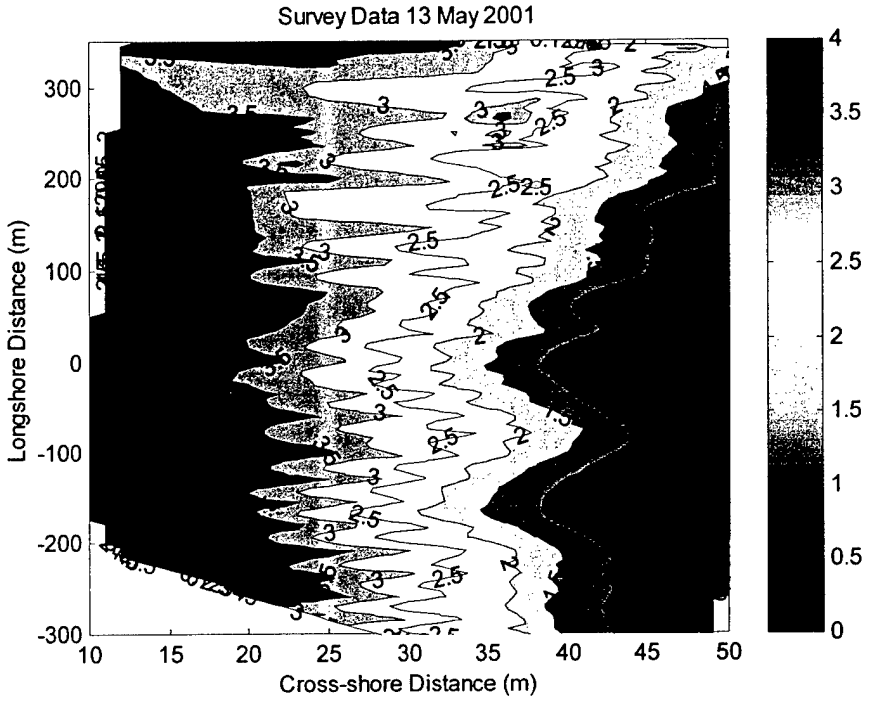
Survey Data 13 May 2001
Longshore Distance (m)
Cross-shore Distance (m)
300
200
100
0
-100
-200
-300
10
15
20
25
30
35
40
45
50
4
3.5
3
2.5
2
1.5
1
0.5
0

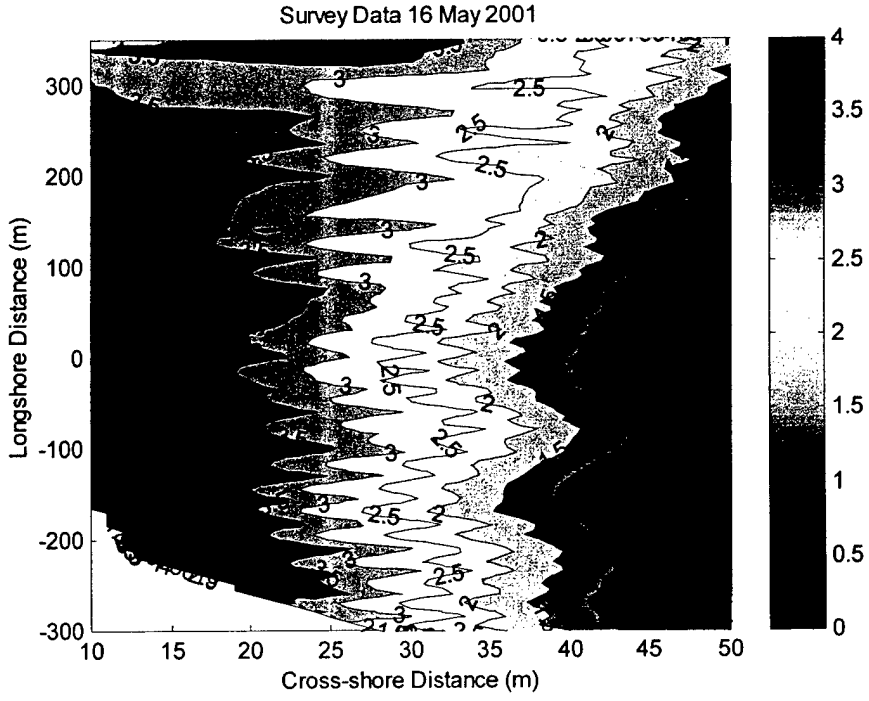
Survey Data 16 May 2001
Longshore Distance (m)
Cross-shore Distance (m)
300
200
100
0
-100
-200
-300
10
15
20
25
30
35
40
45
50
4
3.5
3
2.5
2
1.5
1
0.5
0

REFERENCES

Bagnold, R.A., 1940. Beach formation by waves: some model experiments in a wave tank. *Journal of the Institution of Civil Engineers*, 1, pp. 27-52.

Bascom, W.N., 1951. The relation between sand size and beach face slope. *Transactions of American Geophysical Union*, 32, pp. 866-874.

Battjes, J.A., 1974. Surf similarity. *Proceedings of 14th International Conference on Coastal Engineering*, ASCE, Copenhagen, pp. 466-480.

Bodie, J.G., 1974. Formation and development of beach cusps on Del Monte Beach, Monterey, California. M.S. Thesis, U.S. Naval Postgraduate School, Monterey, California. 66 p.

Bowen, R.J. and Inman, D.L., 1969. Rip Current. *Journal of Geophysical Research*, 74(23), pp. 5479-5490.

Dalrymple, R.A. and Lanan, G.A., 1976. Beach cusps formed by intersecting waves. *Geological Society of America Bulletin*, 82, pp. 5479-5490.

Dean, R.G. and Dalrymple, R.A., 1991. Water Wave Mechanics for Engineers and Scientists. World Scientific, Singapore.

Dean, R.G. and Maurmeyer, E.M., 1980. Beach cusps at Point Reyes and Drakes Bay beaches, California. *Proceedings of 17th International Conference on Coastal Engineering*, ASCE, New York, pp. 863-884.

Dolan, R. and Ferm, J.C., 1968. Crescentic landforms along the Atlantic coast of the United States. *Science*, 159, pp. 627-629.

Dyer, K.R., 1986. Coastal and Estuarine Sediment Dynamics. Wiley and Sons, Chichester.

Eckart, C., 1951. Surface waves on water of variable depth. *Wave Report Number 100.* University of California, Scripps Institution of Oceanography, La Jolla, California. 99 p.

Eliot, I.G. and Clark, D.J., 1986. Observations of bi-spectra of shoaling surface gravity waves. *Journal of Fluid Mechanics*, 161, pp. 425-448.

Escher, B.G., 1937. Experiments on the formation of beach cusps. *Leidse Geologische Mededeelingen*, 9, pp. 79-104.

Evans, O.F., 1939. The classification and origin of beach cusps. *Journal of Geology*, 46(4), pp. 615-627.

Evans, O.F., 1945. Further observations on the origin of beach cusps. *Journal of Geology*, 53, pp. 403-404.

Flemming, N.C., 1964. Tank experiments on the sorting of beach material during cusp formation. *Journal of Sedimentary Petrology*, 34(1), pp. 112-122.

Guza, R.T. and Inman, A.J., 1975. Edge waves and beach cusps. *Journal of Geophysical Research*, 80(21), pp. 2997-3012.

Holland, K.T., 1998. Beach cusp formation and spacings at Duck, USA. *Continental Shelf Research*, 18, pp. 1081-1098.

Holland, K.T. and Holman, R.A., 1996. Field observations of beach cusps and swash motions. *Marine Geology*, 134, pp. 77-93.

Holman, R.A. and Sallenger, Jr., A.H., 1985. Setup and swash on a natural beach. *Journal of Geophysical Research*, 90(C1), pp. 945-953.

Huntley, D.A. and Bowen, A.J., 1978. Beach cusps and edge waves. *Proceedings of 16th International Conference on Coastal Engineering*, ASCE, Hamburg, pp. 1378-1393.

Inman, D.L. and Guza, R.T., 1982. The origin of swash cusps on beaches. *Marine Geology*, 49, pp. 133-148.

Johnson, D.W., 1910. Beach cusps. *Geological Society of America Bulletin*, 21, pp. 604-624.

Komar, P.D., 1971. Nearshore cell circulation and the formation of giant cusps. *Geological Society of America Bulletin*, 82, pp. 2643-2650.

Kuenen, P.H., 1948. The formation of beach cusps. *Journal of Geology*, 56, pp. 34-40.

Longuet-Higgins, M.S. and Parkin, D.W., 1962. Sea waves and beach cusps. *Geological Journal*, 128, pp. 194-201.

Mase, H., 1989. Random wave runup height on gentle slope. *Journal of Waterway, Port, Coastal, and Ocean Engineering*, ASCE, 15(5), pp. 649–661.

Masselink, G., Hegge, B.J. and Pattiaratchi, C.B., 1997. Beach cusp morphodynamics. *Earth Surface Processes and Landforms*, 22, pp. 1139-1155.

Masselink, G. and Pattiaratchi, C.B., 1998. Morphological evolution of beach cusps and associated swash circulation patterns. *Marine Geology*, 146, pp. 93-113.

Nolan, T.J., Kirk, R.M. and Shulmeister, J., 1999. Beach cusp morphology on sand and mixed sand and gravel beaches, South Island, New Zealand. *Marine Geology*, 157, pp. 185-198.

Russel, R.J. and McIntire, W.G., 1965. Beach cusps. *Geological Society of America Bulletin*, 76, pp. 307-320.

Seymour, R.J. and Aubrey, D.G., 1985. Rhythmic beach cusp formation: a conceptual synthesis. *Marine Geology*, 65, pp. 289-304.

Shepard, F.P., 1938. Beach cusps and tides; a discussion. *American Journal of Science*, 235, pp. 309.

Smith, D.H., 1973. Origin and development of beach cusps at Monterey Bay, California. M.S. Thesis, U.S. Naval Postgraduate School, Monterey, California. 67 p.

Takeda, I. and Sunamura, T., 1983. Formation and spacing of beach cusps. *Coastal Engineering in Japan*, 26, pp. 121-135.

Trask, P.D., 1956. Changes in configuration at Point Reyes Beach, California, 1955-1956. *Beach Erosion Board Technical Memorandum*, 91, pp. 61

Werner, B.T. and Fink, T.M., 1993. Beach cusps as self-organized patterns. *Science*, 260, pp. 968-970.

Williams, A.T., 1973. The problem of beach cusp development. *Journal of Sedimentary Petrology*, 43, pp. 857-866.

Wright, L.D., Short, A.D. and Nielson, P., 1982. Morphodynamics of high energy beaches and surf zones: A brief synthesis. Coastal Studies Unit Technical Report Number 82/3, University of Sydney, Sydney, New South Wales.

Wright, L.D., Chappel, B.G., Thom, B.G., Bradshaw, M.P., Cowell, P., 1979. Morphodynamics of reflective and dissipative beach and inshore systems: southeastern Australia. *Marine Geology*, 32, pp. 105-140.